COLLOIDAL CDSE/ZNS, PBSE AND PBS QUANTUM DOTS FOR USE IN APPLICATIONS

A Dissertation

Presented to the Faculty of the Graduate School

of Cornell University

in Partial Fulfillment of the Requirements for the Degree of

Doctor of Philosophy

by

Stephen William Clark

January 2006

COLLOIDAL CDSE/ZNS, PBSE AND PBS QUANTUM DOTS FOR USE IN APPLICATIONS

Stephen William Clark, Ph.D.

Cornell University 2006

Colloidal semiconductor quantum dots are novel materials whose electronic and optical properties can be greatly enhanced from the bulk semiconductor properties by quantum confinement. A brief introduction to colloidal quantum dots and the effect of size on its electronic and optical properties will be given. CdSe/ZnS, PbS, and PbSe quantum dots will be described in more detail with regards to the research done in this dissertation. CdSe/ZnS quantum dots have luminescence that can be tuned in the visible, making them particularly suited for fluorescent labels in biological applications. In particular, their potential use as voltage sensors to detect cell membrane potentials and sphingosine phosphorylation will be discussed. PbS and PbSe quantum dots emit in the near infrared, wavelengths that are important to telecommunications. Their small third-order nonlinearity and relatively long (microsecond) lifetimes will be discussed in terms of dielectric screening. Fluoresence resonant energy transfer between PbS quantum dots will also be discussed.

BIOGRAPHICAL SKETCH

Stephen Clark was born in Illinois in 1976. After high school he attended the University of Illinois at Urbana-Champaign. In 1998, he graduated with a B.S. in Physics. Soon after, he left to attend graduate school at Cornell University in Ithaca, New York.

ACKNOWLEDGEMENTS

I would like to acknowledge my advisor Frank Wise, my committee members Watt Webb and Piet Brouwer, my previous advisors/employers Wilson Ho, John Sullivan, and Thomas Friedmann, my colleagues Andrew Perrella, Jason Petta, Kale Beckwitt, Jeff Harbold, Omer Ilday, Hyungsik Lim, Byun-Ryool Hyun, Yi-Fan Chen, Peer Fisher, Dan Larson, Warren Zipfel and the rest of Webb group, and the rest of the people I worked with, my brother Andrew, my grandparents, and anyone else who would like to be acknowledged.

I would also like to acknowledge the funding support. Most of the CdSe work was sponsored by the Defense Advanced Research Projects Agency under grant MDA972-00-1-0021. The lead salt work was sponsored by Nanoscale Science and Engineering Initiative of the National Science Foundation under NSF Award # EEC-0117770 and the New York State Office of Science, Technology and Academic Research under NYSTAR Contract # C020071. The content of this dissertation does not necessarily reflect the position of the U.S. government, and no official endorsement should be inferred.

TABLE OF CONTENTS

LIST OF TABLES

LIST OF FIGURES

CHAPTER 1

INTRODUCTION

1.1 Colloidal Semiconductor Nanocrystals

Colloidal semiconductor nanocrystals or quantum dots are small pieces of semiconductor that are large enough to still have a crystal lattice but small enough to exhibit quantum confinement effects. Small enough is determined by the Bohr radius of the electron and hole of the bulk semiconductor. The electronic and optical properties begin to change once the size of the nanocrystal becomes small enough to confine the electron or hole.

Semiconductor quantum dots are usually one of two types. Epitaxial quantum dots are grown or patterned on a surface. Colloidal quantum dots are grown in solution from precusors. This thesis will only deal with colloidal quantum dots. There are numerous ways to grow quantum dots in solution. The dots used in this thesis are grown by the injection of organometallic reagents into a hot coordinating solvent. This causes immediate nucleation. The quantum dots continue to increase in size due to the process of Ostwald ripening (smaller nanocrystals are more likely to disolve than the larger ones due to higher surface free energy). The size is determined by when the growth is stopped. This process however does not produce quantum dots of just one size. There is always a distribution of sizes. A common distribution is 5%[1][2]. This distribution will cause the ensemble optical properties to be inhomogenously broadened. Unfortunately, this inhomogenous broadening greatly complicates extracting information on the quantum dots.

Figure 1.1 is a diagram of a general colloidal semiconductor quantum dot. The nanocrystal has a crystal lattice and is often surrounded by optional capping layer

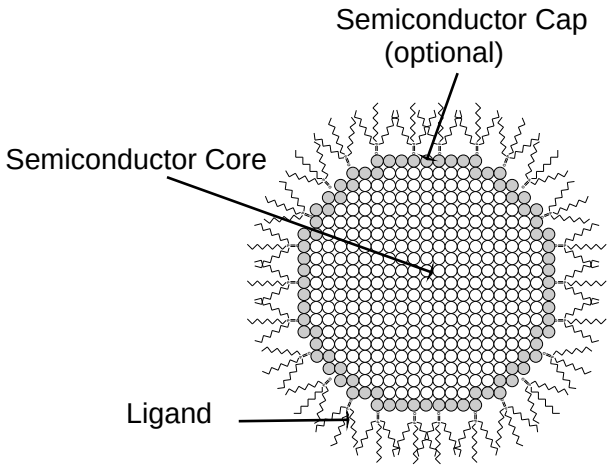

Figure 1.1: Diagram of a general colloidal semiconductor quantum dot

that passivates the surface. Ligands surround the dot and make it soluble. The ligands are also involved in the growth process, but after the growth they can be exchanged. The usual ligand for the dots in this thesis is trioctylphosphine oxide (TOPO), which is soluble in only nonpolar organic solvents. To make the dots water-soluble, the ligands can be exchanged with water-soluble ligands such as oligomeric phosphines[3] or dihydrolipoic acid[4]. Though not shown in the figure, the quantum dots can also be further encapsulated by amphilic molecules. This will be discussed later in the thesis. Note not all colloidal quantum dots are exactly like the figure. The ones studied in this dissertation are.

Theoretical calculations by Efros and Efros[5], Brus[6], and Schmitt-Rink[7] provide a description of the effects that quantum confiment have on the electronic and optical properties of the nanocrystal. By confining the electron or hole, their energy levels are increased and quantized. A simplistic way to view the electronic states of a quantum dot is to first think of the electronic structure of an ideal

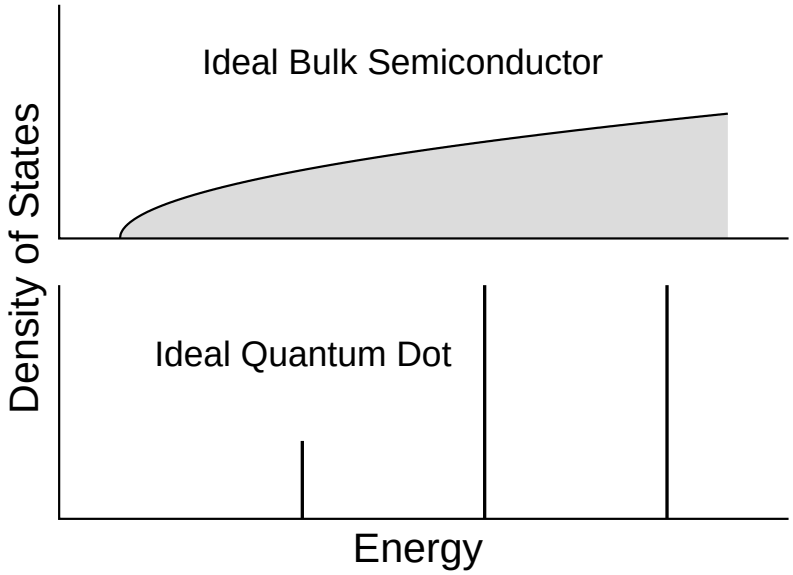

Figure 1.2: Density of states for an electron in an ideal bulk semiconductor (top) and an ideal quantum dot (bottom)

semiconductor. Free electrons in an ideal semiconductor have their energy given by $E \sim \frac{\hbar^2}{2m_e}\left(k_x^2 + k_y^2 + k_z^2\right)$. The k values are quantized to be an integer multiple of $\frac{\pi}{L}$ for a semiconductor in an infinite potential (or $\frac{2\pi}{L}$ if using periodic boundary conditions), where L is the length of the semiconductor. For a bulk semiconductor, L is a macroscopic distance. Thus the energy levels are so closely spaced as to make the energy almost a continuous function of k. This yields the familiar density of states shown in the top of Figure 1.2 which is proportional to the square root of the energy.

As L becomes smaller, the energy spacing becomes larger such that the energy levels can no longer be considered continuous. The density of states then becomes quantized as shown in the bottom of Figure 1.2. The smallest energy level, which is given when the k values are the smallest nonzero multiple of $\frac{\pi}{L}$, also increases by an amount of $\frac{\pi^2\hbar^2}{2mL^2}$ from the bulk lowest energy level. The energy levels of the

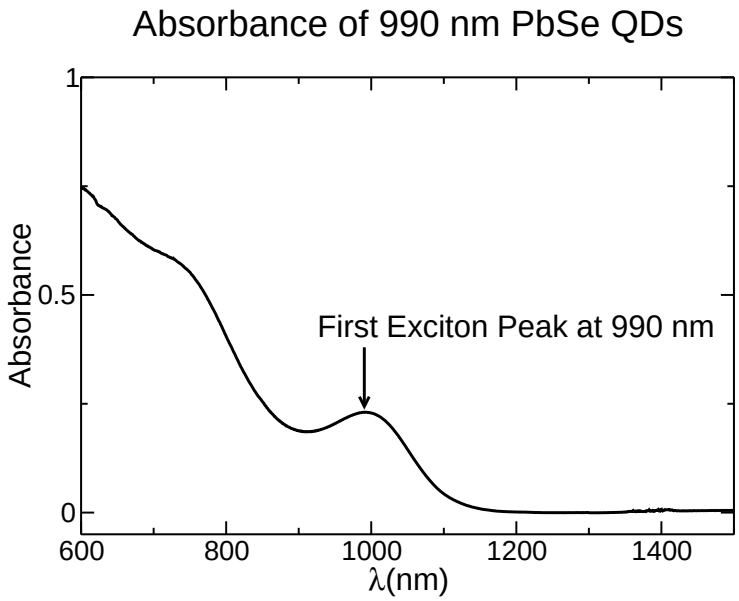

Figure 1.3: Absorbance of a typical sample of PbSe quantum dots. The first exciton peak is clearly visible at 990 nm.

holes in the ideal semiconductor are quantized the same way, with m_h, the effective mass of the holes, replacing m_e, the effective mass of the electrons.

While this model is overly simplistic, it does explain the discreteness of the states and the fact that the states become more separated as the size decreases, and that the lowest energy level shifts on the order of L^{-2}. While colloidal quantum dots can be grown in many shapes, they are usually spherical in shape. All the quantum dots in this thesis are spherical. Therefore the electronic states are not labelled by cartesian quantum numbers, but by the spherical quantum numbers s, p, d, etc. Also, the energy levels have a small homogenous linewidth and measurements of an ensemble of quantum dots also will have large inhomogenous broadening due to the size distribution of the quantum dots.

Figure 1.3 is the absorbance of a typical sample of PbSe quantum dots studied in this thesis. One can see discrete states in the absorbance, though they are

clearly inhomogenously broadened. The lowest energy level is clearly seen and it is labeled as the first exciton peak. The first exciton peak is the transition from the unexcited state of the semiconductor to having one electron in the lowest electron state, the s_e state and one hole in the lowest hole state, the s_h state. Throughout this thesis quantum dots will either be denoted by the peak of the luminescence or the peak of first exciton. For example the plots in later chapters that just denote PbS quantum dots with 770 nm absorbance, imply that the quantum dots have its first exciton peak at 770 nm. It will of course have a very broad absorption.

Much more realistic treatments require knowledge of the actual band structure of the semiconductor. Therefore, while the semiconductor quantum dots will all roughly have the general characteristics described above, the actual electronic structure will differ between each semiconductor. When dealing with the actual electronic structure, semiconductor quantum dots are separated into three confinement regimes.

In the weak confinement regime the size of the quantum dot is larger than both the Bohr radius of the electron and the hole. The exciton created in this type of quantum dot acts much like an exciton in the bulk. In the intermediate confinement regime, only the electron is confined. When both the electron and hole are confined, both the electron and hole have their energy levels increased and quantized. This is referred to as strong confinement. Semiconductor quantum dots with strong confinement exhibit the greatest enhancement in optical properties. Whether a semiconductor system can exhibit intermediate or strong confinement depends mainly on the properties of the bulk semiconductor, as the smallest quantum dot that can be grown is still a few lattice constants in size. In some semiconductors the Bohr radius for the electron or hole will be too small to

be confined in a quantum dot that can be realistically grown.

Quantum dots have many useful optical qualities. Because the states are quantized, the dipole strengths are greatly increased from the bulk. Also, as long as the surface of the quantum dot is well passivated such that there are no traps for either electrons or holes, the quantum yield should be higher than in the bulk, as the electron and hole can not drift away from each other as in the bulk.

Though the energy levels are quantized, there is still many of them. This gives quantum dots a characteristically broad absorption. The quantum dots studied in this dissertation all relax to the lowest energy state before emitting. This gives them a characteristically narrow emission. While a broad absorption and narrow emission is similar to the bulk semiconductor, this property is quite different from usual fluorophores such as dyes, As quantum dots are often compared with fluorophores such as dyes, it is important to note the difference.

Since the lowest energy level is determined by the confinement, the emission wavelength can be tuned by the size. This allows for semiconductor nanocrystals, all of which have the same chemical composition, to span a wavelength range. The long wavelength is determined by the bandgap of the bulk, though there is no enhancement for dots that are this size. The short wavelength is determined by the size necessary to make a crystal lattice, usually 1-2 nm[1].

There are many semiconductor systems that can be made into colloidal quantum dots. In this thesis we will look at two different wavelength regions. The visible, which is useful for biological imaging, is covered by the CdSe quantum dots. The CdSe quantum dots however only have intermediate confinement. Only the electron is confined by the size. The hole is unaffected. It is common for the CdSe quantum dots to have a ZnS cap to improve the quantum yield because of

better surface passivation from the ZnS as opposed to the ligands.

The PbS and PbSe dots span the near-infrared which is the useful range for telecommunications. Both the PbS and PbSe quantum dots are strongly confined. While PbSe can have a higher band gap semiconductor cap[8], in this work the PbS and PbSe quantum dots without a cap are used.

1.2 Organization of the Dissertation

This dissertation is divided roughly into two parts. The first discusses research done with the CdSe/ZnS quantum dots. This part will include a quick introduction along with attempts to put the quantum dots inside cell membranes and model membrane systems in chapter two. Chapter three will include a part on the encapsulation of the quantum dots with sphingosine in an attempt to detect phosphorylation of the sphingosine. The final chapter on CdSe/ZnS quantum dots, chapter four, will discuss a final attempt at membrane potential detection and conclude the work with CdSe/ZnS.

The second part discusses the research done with the lead salt, PbS and PbSe, quantum dots. The fifth chapter will pertain to measuring the nonlinearity of the lead salts. After that the lifetime of PbS quantum dots will be discussed and the implications for the dielectric screening model will be covered. Then fluorescence resonant energy transfer between the PbS quantum dots will be covered last of all.

CHAPTER 2

CDSE/ZNS QUANTUM DOTS IN BIOLOGY

2.1 Introduction

CdSe has a bulk bandgap of 730 nm[9]. Quantum confinement can make the first resonance from the bulk all the way down to 400 nm [1][10][11]. This makes them useful as fluorophores for biological imaging [12][13][14]. As mentioned in the introduction, the CdSe quantum dots do not exhibit strong confinement. Only the electrons are confined by the quantum dot, not the holes. CdSe quantum dots usually have a capping layer of ZnS. The ZnS passivates the surface better than the ligand, and thus it increases the quantum yield. A diagram of a CdSe quantum dot is in Figure 2.1.

CdSe/ZnS quantum dots have the characteristic narrow emission and broad excitation of semiconductor nanocrystals. For comparison, in Figure 2.2 the excitation and emission of green emitting CdSe/ZnS quantum dots is compared with a standard dye, Rhodamine B. This fact, coupled with the fact that the emission wavelength is tunable by size without changing the chemical makeup of the surface or dot, make them ideal for multicolor imaging[15]. They have also been shown to exhibit a large Stark shift[16][17][18][19].

To use quantum dots in biological applications, they have to be made water-soluble. As made, the quantum dots are covered in a hydrophobic ligand, usually trioctylphosphine oxide (TOPO). This ligand is used in the growth process and allows the quantum dot to be soluble in nonpolar organic solvents. Early on, making the quantum dots water-soluble proved to be quite difficult. When this research was started, this problem was just being solved. Quantum dots can be made

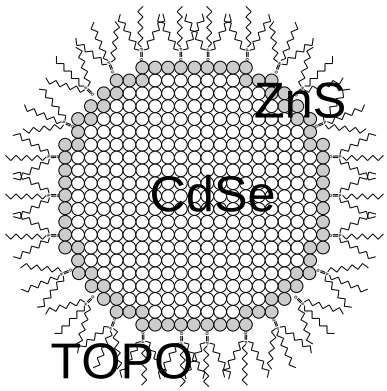

Figure 2.1: Diagram of a CdSe/ZnS quantum dot

water-soluble by coating them in silica coat[12], exchanging the TOPO molecule for a water-soluble ligand[13][4], or encapsulating the TOPO covered dot with an amphilic polymer[20] or lipid[14]. The water-solubility issue is now considered solved. Water-soluble CdSe/ZnS quantum dots are now commercially available. Nonetheless, both organic-soluble quantum dots and water-soluble quantum dots were studied. The quantum dots used in this chapter were provided by Marcel Bruchez of Quantum Dot Corporation of Hayward, California.

2.2 Initial Characterization

Before research began into using the quantum dots as voltage sensors, an initial characterization of the dots was performed. The CdSe/ZnS quantum dots have been known to be bright fluorescent biological labels[12][13]. Unfortunately, they were also known to blink[21]. Their fluorescence would turn on and off randomly when excited. This property is undesireable especially in potential applications that require single molecule tracking. These qualities of the quantum dot were

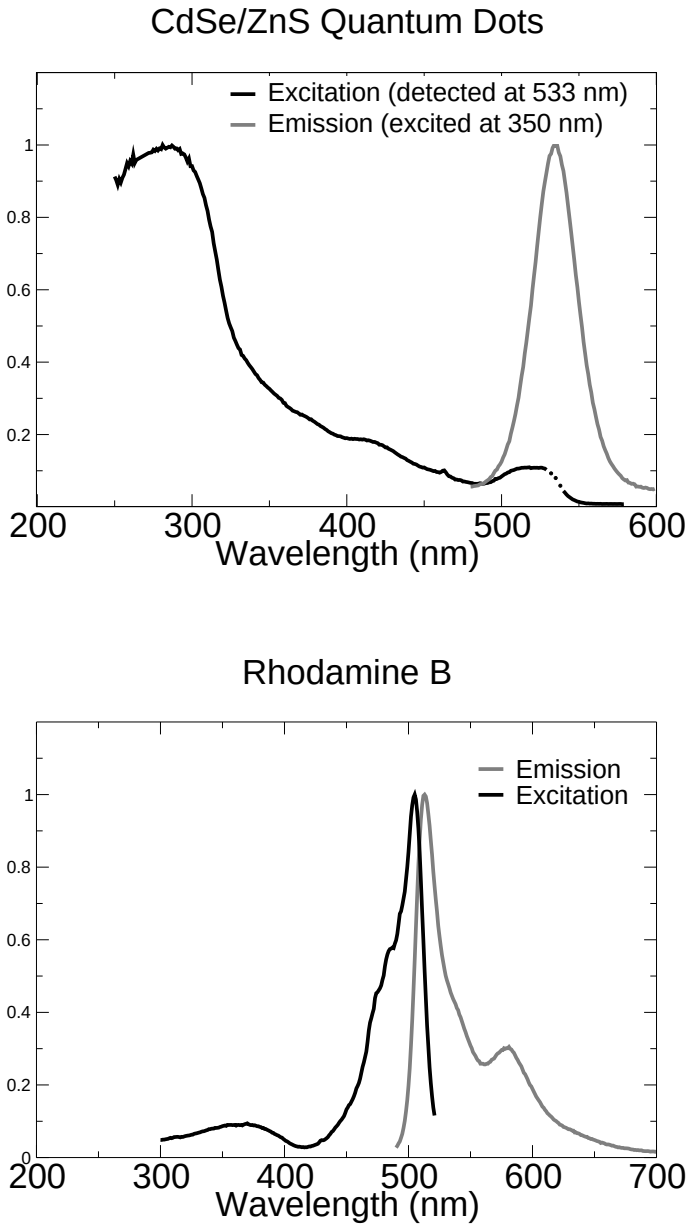

Figure 2.2: Top: CdSe/ZnS Photoluminscence Excitation and Emission; Bottom: Rhodamine B Photoluminscence Excitation and Emission for comparison

desired to be characterized with fluorescence correlation spectroscopy (FCS). As this initial characterization is already well reported in publication[22] and Dan Larson's thesis[23], only a summary of the results will be given here. Both the organic-soluble and water-soluble dots were used in this study. The quantum dots were made water-soluble by coating the dot with an amphilic polymer as described in Reference [20].

FCS is a relatively straightforward experiment. A recent review of FCS is given in Reference [24]. An optical focal volume of less than a femtoliter is setup inside a solution containing the fluorophores. The fluorophores diffuse into and out of the focal volume by Brownian motion. The experiment is setup such that only fluorophores that are in the focal volume are both excited and have their fluorescence collected. The data taken is just photons counted versus time. A typical trace is shown in the top of Figure 2.3. The fluctuations in the data are mainly the effect of diffusion. The actual FCS curve is just the normalized autocorrelation of the photons counted versus time trace. A theoretical FCS curve for a fluorophore that experiences only simple diffusion is shown in the bottom of Figure 2.3.

For the case of simple diffusion, the curve shown in bottom of Figure 2.3 indicates two properties. The photons are only correlated for the time it takes for the fluorophore to diffuse through the focal volume. Thus by knowing the dimensions of the focal volume, the diffusion coefficient can be measured. Also the amount of correlation is equal to $1/N$ where N is the number of emitting fluorophores in the focal volume. The concentration can then be determined. For the full theoretical treatment see Dan Larson's thesis[23] and references therein.

FCS can however show much more than just concentration and diffusion coef-

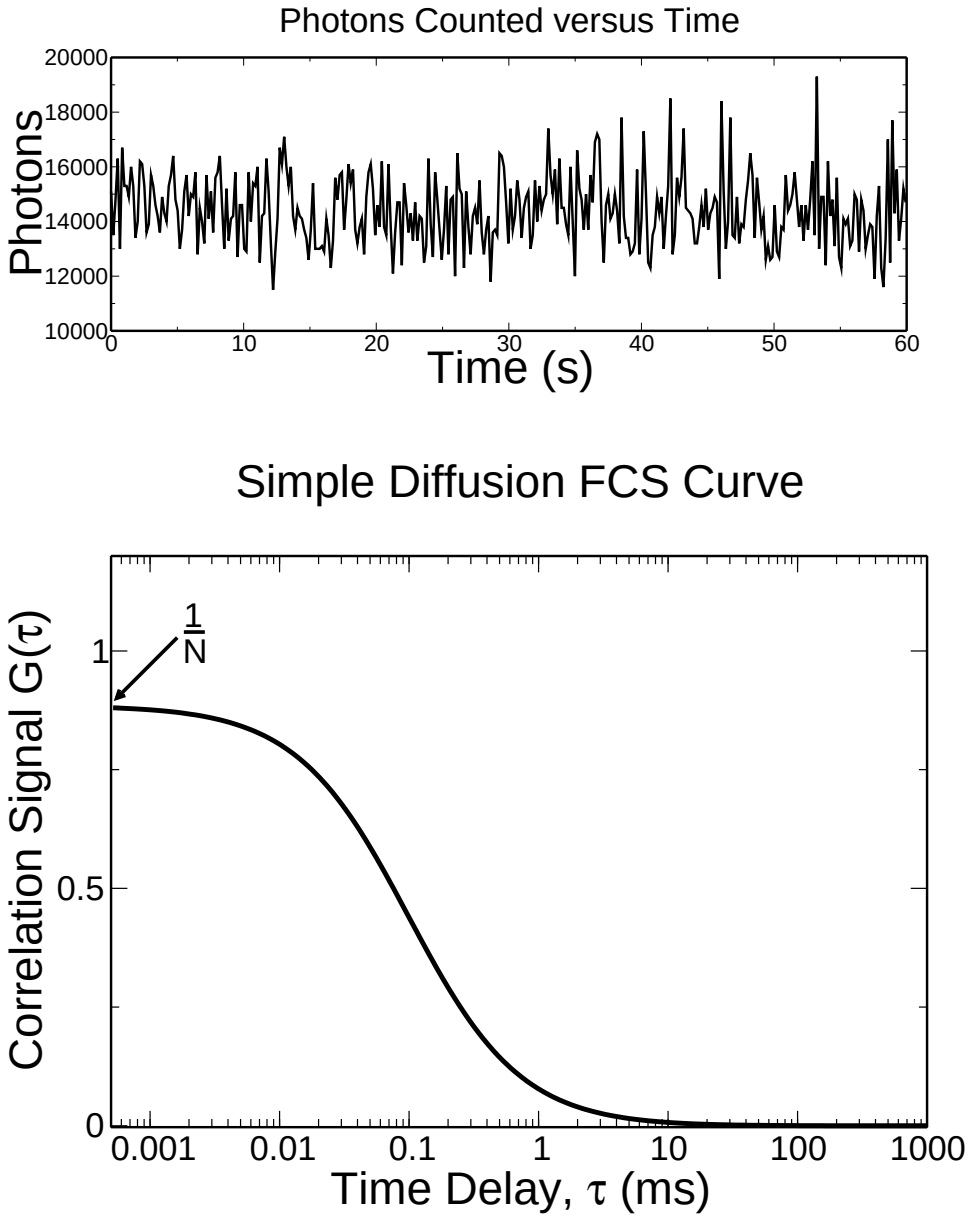

Figure 2.3: Top: Sample trace of photons counted versus time for a typical FCS experiment. Bottom: Theoretical FCS curve for simple diffusion

ficients. Processes that affect the fluorescence of the particle that happen on time scales smaller than the diffusion time scale can also be seen. Blinking, such as a dye going into a non-emitting triplet state, can be seen if the blinking time (the triplet lifetime in this case) is less than the diffusion time. This is because amount of correlation, $1/N$, is the number of *emitting* fluorophores. If the fluorophores can go from a nonemitting state to an emitting state on a time scale smaller than diffusion, then the amount of correlation will show that change. Photobleaching can be seen as an excitation intensity dependent change in the apparent diffusion time. There is no correlation between photons after a fluorophore has been bleached as well as when it diffuses out of the focal volume.

If the solution being studied is made of more than one fluorophore, each with greatly different diffusion coefficients, FCS will also be able to show this. This was not an issue with this study of quantum dots, as the quantum dots did not aggregate and were quite monodisperse. In the next chapter of this thesis, however, single quantum dots will be encapsulated in lipid micelles to make them water soluble. FCS serves as a great diagnostic in that case, as it can easily determine if the micelle encapsulates just one quantum dot or many.

The FCS experiment provided significant insight into the quantum dots. FCS of the quantum dots showed an apparent concentration increase versus excitation intensity. This was explained as an saturation of absorption which made the dimensions of the focal volume effectively increase with excitation intensity. Equally important is that FCS measured the diffusion of the quantum dots. The diffusion measurements showed that the quantum dots had a much larger hydrodynamic radius than expected. In other words, quantum dots diffuse slower than hard spheres of the same size. Quantum dots soluble in nonpolar organic solvents that were only

5 nm in diameter have a 9 nm hydrodynamic radius. For water-soluble dots which have an amphilic polymer layer over the TOPO ligands[20], the hydrodynamic radius was 14 nm.

The hydrodynamic radius is significant, not that the radius represents an actual size, but that attaching the dots to biological molecules will affect their movement more than previously thought. It is also of note that the larger than expected hydrodynamic radius had been mentioned in an early study by Mattoussi and coworkers [25].

FCS also showed no blinking on the millisecond (diffusion) timescale in solution. However, later research by others[26] indicated that conclusion to be incorrect. The dots still blink even in solution. The reason for the different conclusion as explained by the researchers was that the autocorrelation function would not be able to distinguish the blinking of quantum dots because the blinking has a power-law distribution[27].

2.3 Membrane Potential Measurements

There is a desire in neuroscience to be able to do real-time imaging of electrical signaling in cellular systems such as neurons. To do so, fluorophores are required that are bright, photostable, nontoxic, and have a large, fast change in fluorescence in the presence of an electric field. A typical membrane is 4 nm across with a maximum voltage of 100 mV. This means that the fluorophore must be able to have a measurable change in signal at 250 kV/cm. The change should also take place in less than 1 ms. Voltage sensing fluorophores usually fall into two categories. One relies on molecular reorientation or redistribution in the presence of an electric field. This is slow process, but often produces very large shifts in fluorescence[28].

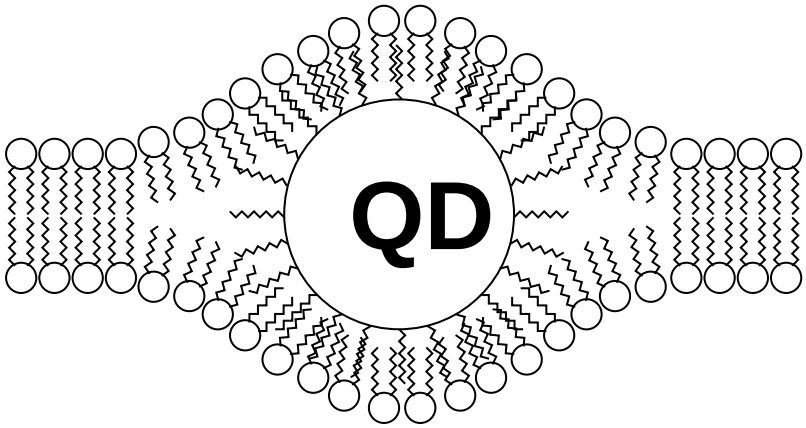

Figure 2.4: Schematic of a quantum dot inside a lipid bilayer. Figure roughly to scale.

The other rely on an electrochromic effect that is fast, but often not very large[29].

2.4 Stark Effect Measurements

Earlier studies by Colvin and coworkers [16][17][18] and Empedocles and coworkers [19] indicated that the quantum dots have a large Stark Effect. The Empedocles study measured a quadratic luminescence shift for single CdSe/ZnS the order of 40 meV at 250 kV/cm. This study was with single dots on a glass slide at 10 K. Also of note, Empedocles and coworkers measured this shift for CdSe dots with a ZnS capping layer. One may have thought that the ZnS capping layer would provide some screening of the electric field and that was not the case.

Given the large measured Stark shift of the quantum dots, the purpose of our study was to see if the quantum dots could detect changes in cellular membrane potential. This required the solution to two distinct problems. First was whether or not quantum dots could be put inside membranes. A typical membrane is only 4 nm thick, while a typical dot is around 5 nm in diameter not including the

ligands. Figure 2.4 shows a diagram of the relative sizes of a quantum dot and a lipid bilayer. Needless to say, a quantum dot will greatly perturb a biological membrane.

The next question is whether the dots would still be sensitive to voltage changes. The roughly 250 kV/cm maximum field across a membrane is based on the roughly 100 mV potential over 4 nm. With the membrane perturbed to be almost 10 nm thick with the dot, a reduction of 2.5 can be reasonably expected in field. Also, since the dots have to be modified to make them water soluble, there is a question of whether that will cause screening effects.

2.5 Black Lipid Membranes

The first attempt to study these problems were with black lipid membranes (BLM) [30]. Black lipid membranes are simple model membrane systems that are suspended over a hole in a plastic sheet in salt water. Electrodes can be put in the salt water on both sides of the membrane, and thus control the voltage across the membrane. This system should allow the study of quantum dots in a bilayer.

The method is as follows. Egg Phosphatydilcholine acquired from Avanti Polar Lipids was dissolved in decane. The plastic support was made of a thin peice of polyethylene. A hole was made in the center by use of a hot (>100 C) needle brought close, but without touching the plastic. The hot needle was removed when the hole was just less than 1 mm in diameter as seen by eye. Then the plastic support was immersed in salt water. The lipid decane mixture was "painted" or spread over the hole. The lipid mixture then begins to thin to a bilayer.

Since quantum dots in their usual form are soluble in nonpolar organic solvents such as decane, it was hoped that by putting the quantum dots in the lipid-

decane mixture would protect them from the water. Water-soluble quantum dots can't be used, because they are surrounded by hydrophilic molecules, and would immediately leave the bilayer. Quantum dots soluble in nonpolar organic solvents can't be put into the water after the BLM has thinned because the dots are very hydrophobic and will immediately aggregate.

The end result, however, was that the lipid-decane-QD mixture when "painted" over the hole in the plastic would not thin to a bilayer. Thus no membrane potential experiment could be done. This work was done with the help of Professor Peter Hinkle from the Molecular Biology and Genetics department at Cornell University.

2.6 Giant Unilamellar Vesicles

In the hopes that another model membrane system would work, the membrane system of giant unilamellar vesicles was tried. A unilamellar vesicle is a single lipid bilayer that has formed the shape of a sphere. The giant refers to it being greater than 10 μm. The purpose was to try an experiment similar to that done by Jerome Mertz and coworkers[31]. This involves putting a GUV between two electrodes. An AC field is put between the electrodes and due to the mobility of ions inside the GUV near the bilayer, a field is produced on certain parts of the GUV. This is a much more complex experiment than the BLM.

GUVs were formed using either the method of electroswelling[32] or by the method of hydration after evaporation[33]. The electroswelling method requires drying lipids out in chloroform on large sheets of indium tin oxide (ITO). Then placing the sheets of ITO together space about 1 mm apart and filling the area with 50 mM sucrose solution. Then an AC field of 2 V at 5 Hz is applied for 2 hours and the GUVs form. The other method merely requires lipids to be evaporated

in a Teflon or glass tube. Then they are slowly hydrated in a humid incubator at 37 C. The electroswelling method produced better vesicles in terms of uniformity.

The same issue of whether to use quantum dots that are soluble in nonpolar organic solvents or water-soluble quantum dots is considered. Again since lipids and quantum dots both dissolve in organic solvents, the method tried was to dissolve the quantum dots and lipids together in chloroform. The chloroform mixture was then evaporated onto the ITO plates. The rest of the procedure was then followed to try to form the GUVs. Unfortunately, while GUVs would form, none of the quantum dots would be inside the bilayer of the GUVs. Because of this, the experiment similar to Reference [31] was never setup or tried. This work was done with the help of Tobias Baumgart of the Webb group.

2.7 Rat Basophilic Leukemia Cells and Gramicidin

Another attempt was made but now using an already stable cellular system. The Rat Basophilic Leukemia (RBL) cells are a standard model cell that is easily grown in Webb group lab. Upon introduction of gramicidin to RBL cells, their usually large negative membrane potential quickly reduces to zero[34][35].

RBL cells were grown on thin plastic sheets in the Webb lab. After switching the cells from a growth medium to Tyrodes buffer with glucose, the sheets were then cut and put into a cuvette. The cuvette was placed in the sample compartment of a PTI fluorometer, and the fluorescence was monitored. The dye used in References [34][35], bisoxonol, was tried first. Bisoxonol easily goes into the RBL membrane after it is introduced into water. Unlike an organic-soluble quantum dot, it is only slightly hydrophobic. Upon introduction of gramicidin to the RBL cells, the fluorescence of the bisoxonol greatly increased as expected.

The water-soluble dots were used this time, as there was no way to get the organic-soluble quantum dots into the RBL cells without them aggregating. While it was realized that the water-soluble dots would not go into the membrane, it was hoped that some would stick to the membrane and be close enough to be affected by the electric field. This was not the case, the quantum dots had no affinity towards the cells.

2.8 Conclusion

The end result was that none of these methods worked. The model membrane systems of the giant unilamellar vesicles and black lipid membranes would not form with quantum dots in them. The RBL cells were very difficult to get quantum dots to stick to, and they did not show any sign of a fluorescence change with the addition of gramicidin. Possible reasons for this failure will be discussed in a later chapter.

CHAPTER 3

CDSE/ZNS QUANTUM DOTS FOR STUDIES OF SPHINGOLIPID METABOLISM

3.1 Sphingolipid Metabolism

With the membrane potential measurements providing no results, a new idea was set forth by professor David Russell of the Microbiology and Immunology department of the College of Veterinary Medicine at Cornell. His idea was to encapsulate quantum dots not in a bilayer, but in a spherical micelle. Then by changing the charge on lipids encapsulating the quantum dot, perhaps the quantum dot would have its luminescence shift due to the change in electric field. Around the same time a research paper was published by a Dubertret and coworkers at Rockefeller University, that successfully encapsulated quantum dots in a spherical micelle with a mixture of lipids to make the quantum dots water-soluble[14].

The lipids to be studied in this research were the sphingolipids. The sphingolipids are an important class of lipids involved in the signal transduction pathways that mediate cell growth, differentation, and death. Sphingosine is the most common backbone of the sphingolipids, and the phosphorylation of sphingosine is an important step in sphingolipid metabolism[36].

The specific process that is desired to be studied is the phosphorylation of sphingosine into sphingosine-1-phosphate. Phosphorylation is the addition of a charged phosphate group to a lipid. The phosphorylation of sphingosine requires the enzyme sphingosine kinase and adenosine triphosphate (ATP). The enzyme takes a phosphate group from the ATP and attaches it to the sphingosine. The ATP becomes adenosine diphosphate (ADP) and the sphingosine becomes the

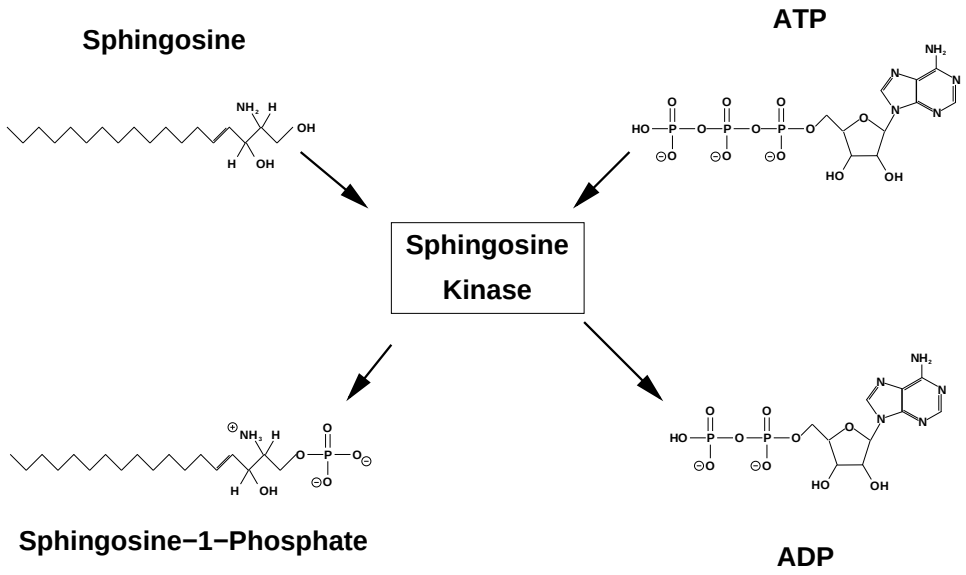

Figure 3.1: Diagram of Sphingosine Phosphorylation

negatively charged sphingosine-1-phosphate. Figure 3.1 is a diagram of the process.

Figure 3.2 is diagram of a quantum dot with a phosphorylated sphingosine lipid on it. The figure is roughly to scale. The electric field from one charge at 10 nm is roughly 140 kV/cm, which should large enough for the quantum dot to be affected. A key difference between this case and the membrane potential measurements is that in this case the charges from phosphorylation may be uniformly spread across the surface of the quantum dot as opposed to producing a electric field across the quantum dot as with the membrane.

The desired goal is to use encapsulated quantum dots as a monitor of the enzyme activity. Once one has such a monitor, then one can conceivably study such things as the time response of the enzyme and substances that may affect the activity of the enzyme.

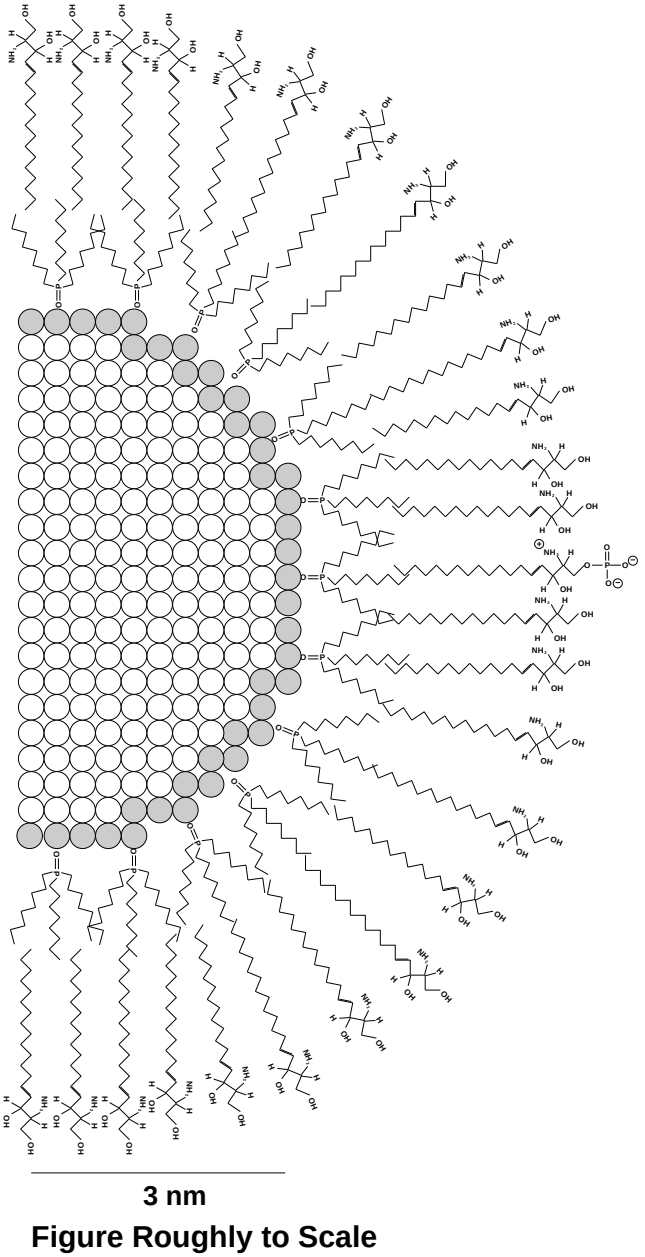

Figure 3.2: Diagram of quantum dot with one sphingosine phosphorylated to sphingosine-1-phosphate. Figure roughly to scale.

3.2 Encapsulating Quantum Dots with Sphingosine

Dubertret and coworkers were able to encapsulate quantum dots in a mixture of dipalmitoyl phosphatidylethanolamine-polyethylene glycol (DPPE-PEG) and dipalmitolyphosphatidylcholine (DPPC). Both DPPE-PEG and DPPC are lipids with fully saturated double hydrocarbon chains of 16 unit length. While they tried several different lipid combinations, they concluded that both the PEG and a double hydrocarbon chain found on the DPPE were needed. However, a lot is known about the self-assembly of lipids[37][38][39], and using that knowledge one should be able to change the method of Dubertret and coworkers to use sphingosine.

There are three characteristics a lipid must have to form a micelle[37][38][39]. The first is that the lipid must be amphilic, which means it must have both a hydrophilic part, the polar headgroup, and a hydrophobic part, the hydrocarbon chain. Since there is no chemical bond between the hydrocarbon chains, the hydrophobic part must be large enough to make the structure stable. Technically, this means the lipid must have a low critical micelle concentration (CMC). The CMC is the concentration at which the lipids will start to self-assemble into structures. If the concentration is below the CMC, the lipids will just exist separately in solution.

The CMC is given generally by the equation CMC$\approx \exp[-(\mu_1^0 - \mu_N^0)/k_BT]$. The factor k_BT is Boltzmann's constant multiplied by the temperature. The constant μ_1^0 is the standard part of the chemical potential or the mean interaction free energy per molecule for single molecules in solution. Likewise μ_N^0 is for the aggregate of molecules, in this case a micelle. N is just the number of molecules in the aggregate[37]. Unlike the difference between the chemical potentials, the CMC is easily measured. Thus the discussion will use the CMC as the measure

of stability or affinity between the lipids, though there is no real chemical bond or attractive force. The lower the CMC, the greater the difference between the chemical potentials of the single molecule with respect to the micelle. This then implies greater stability of the micelle structure.

The CMC of an amphilic molecule depends on the size of hydrophobic hydrocarbon chains with respect to the size of the hydrophilic part. Lipids usually have either one or two hydrocarbon chains. Those with two hydrocarbon chains have a much lower CMC. Also by increasing the length of the chain, the CMC goes down as well. For some typical numbers, a phosphatidylcholine (PC) with a double 5 unit hydrocarbon chain has a CMC of 90 mM. One with a double 10 unit chain has a CMC of .005 mM. And a PC with just a single 10 unit chain has a CMC of 8 mM[40].

The second characteristic needed is that the lipid must also have the proper packing geometry to form a micelle as opposed to other structures, such as the more common bilayer. The measure used here is the critical packing parameter (CPP). The CPP of a amphilic molecule is defined as the volume (v) of the hydrocarbon chains divided by the product of the area of the head group (a) and the length of the hydrocarbon chain (l), or CPP$= v/al$. For a micelle to form, the CPP must be at or below one third. This can be seen by just dividing the volume of a sphere by its surface area and radius. For a bilayer, the CPP must be around one. Thus the CPP is a measure of the curvature of the structure the amphilic molecule will form. For example, if one wanted to encapsulate a sphere of diameter 5 nm with lipids of hydrocarbon length 2 nm, the volume of the hydrocarbon chains would have to be $v = \frac{4}{3}\pi((2.5+2)^3 - 2.5^3)$. The surface area would have to be $a = 4\pi(2.5+2)^2$. This would require a molecule with a CPP of 0.62.

The last characteristic is that there must be some sort of repulsive interaction to keep the encapsulated dots from aggregating. It is important to note however that the actual self-assembly dynamics are much more complex. This simple version neglects several important properties. The phase transition temperature of the lipids is an important property that is neglected. This affects the volume of the hydrocarbon chains. The effect of salt and pH on the lipids is also important. Salt can screen charges on the headgroups of the lipids which will decrease the surface area of the head groups. Also changes in pH can actually change the charge on the head groups as well. Also since the hydrocarbon chains aren't rigid, the CPP is not really an exact requirement. It is more of a guideline. However, this simple version of self-assembly dynamics is more than good enough to provide a starting point in picking lipids and rules of thumb in deciding how to adjust the procedure.

Often however, it is difficult to have all the necessary characteristics to form micelles with low CMCs met at the same time. For instance DPPC, which is one of the shorter chain length components of GUVs, BLMs, and cellular membranes, has a very low CMC, 4.6×10^{-10}M [40]. This fact makes cellular membranes very stable. Unfortunately, its geometry is such that it forms bilayers. Not surprisingly, Dubertret and coworkers were unable to form micelles with DPPC alone. Usually lipids that form micelles usually have either very short double hydrocarbon chains or short single hydrocarbon chains, and therefore they usually have CMCs in the millimolar range. DPPE-PEG is an exception as it has a long double hydrocarbon chains that give it a CMC of 70 μM[41]. A mixture of DPPC and DPPE-PEG will lower the CMC still, though it will increase the overall average CPP. As previously calculated, the CPP for encapsulating a quantum dot ($\sim$0.6) is more than is required for a micelle ($\sim$0.33), so the addition of DPPC should be beneficial.

The DPPE-PEG lipid also has the steric hindrance from the PEG. This keeps not only biomolecules from sticking to the quantum dots, but also keeps the quantum dots from sticking to each other.

When trying to encapsulate dots with sphingosine, different lipids were tried besides DPPE-PEG. It was feared that the steric hindrance of the PEG might interfere with the enzyme. That concern coupled with an initial difficulty in getting the DPPE-PEG/DPPC encapsulation to work, caused other lipids to be tried first. As seen in Figure 3.1 sphingosine has no real head group and is therefore very hydrophobic. The quantum dots are covered with trioctylphosphine oxide (TOPO), which is also very hydrophobic. TOPO has a triple hydrocarbon chain, with each chain is 8 units long. Trying to encapsulate quantum dots in sphingosine alone doesn't work. The sphingosine and quantum dots just clump together and aggregate out of solution. Therefore a mixture of lipids is required.

It is known that 12 unit single chain PC forms micelles[42] as well as 7 unit double chain PC[43]. These would be the limit the lower end of the chain length, as they have high CMCs and low CPPs. Due to price considerations, not all lipid combinations can be tried and the PC lipids are often the cheapest. Since the CPP of the encapsulating lipids should be higher than required for micelle formation, slightly longer lipids can be used to lower the CMC. As for a repulsive interaction, adding a small amount of charged lipids will keep the quantum dots from aggregating. The charged lipids choosen where the phosphatic acid (PA) lipids which are similar to the PC except they are missing the choline group (the nitrogen and hydrocarbons) attached to the phosphate group making it negative, and ethylphosphatidylcholine (EPC) which is PC with the phosphate neutralized making it a positive lipid.

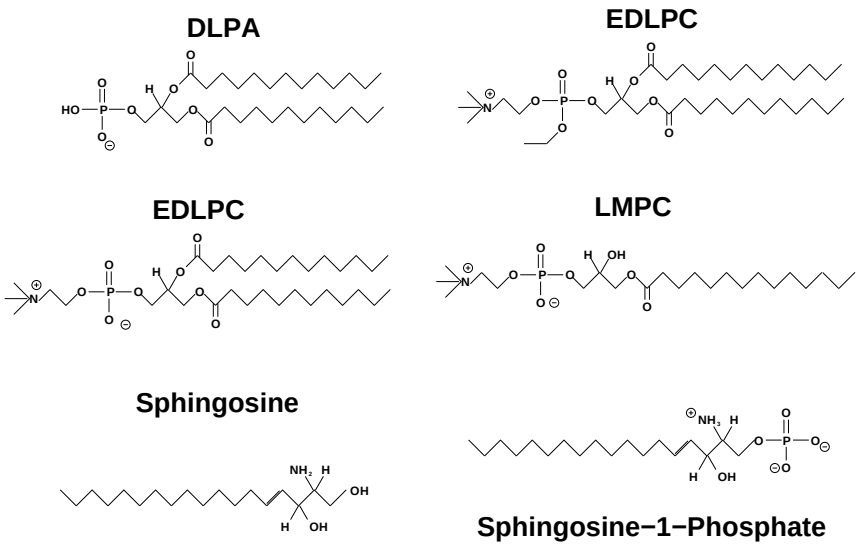

Figure 3.3: Chemical structure of the lipids used to encapsulate the quantum dots.

The appendix has the methodology and exact lipid combinations tried. Using just lysomyristoyl phosphatidylcholine (LMPC), dilauroyl phosphatidylcholine (DLPC), dilauroyl ethylphosphatidylcholine (EDPLC), and dilauroyl phosphatic acid (DLPA) with the sphingosine, quantum dots were successfully encapsulated and made water-soluble. The LMPC is has single 14 unit hydrocarbon chain while the DLPC, EDPLC, and DLPA have double 12 unit hydrocarbon chains.

Figure 3.3 shows the chemical structure of the lipids used. Sphingosine content ranged from 5 to 90 percent. FCS was used to make sure that the prepared dots were in fact monodisperse. Two such curves are shown in Figure 3.4. The fact that the curves fit a single diffusion curve and the hydrodynamic radius is similar to quantum dots measured in the previous chapter, implies that they are in single dot micelles and are not aggregated. Stability was never measured accurately. Quantum dots encapsulated without a charged lipid would start to aggregate within days. Quantum dots with charged lipid would last around 2 weeks. Therefore the

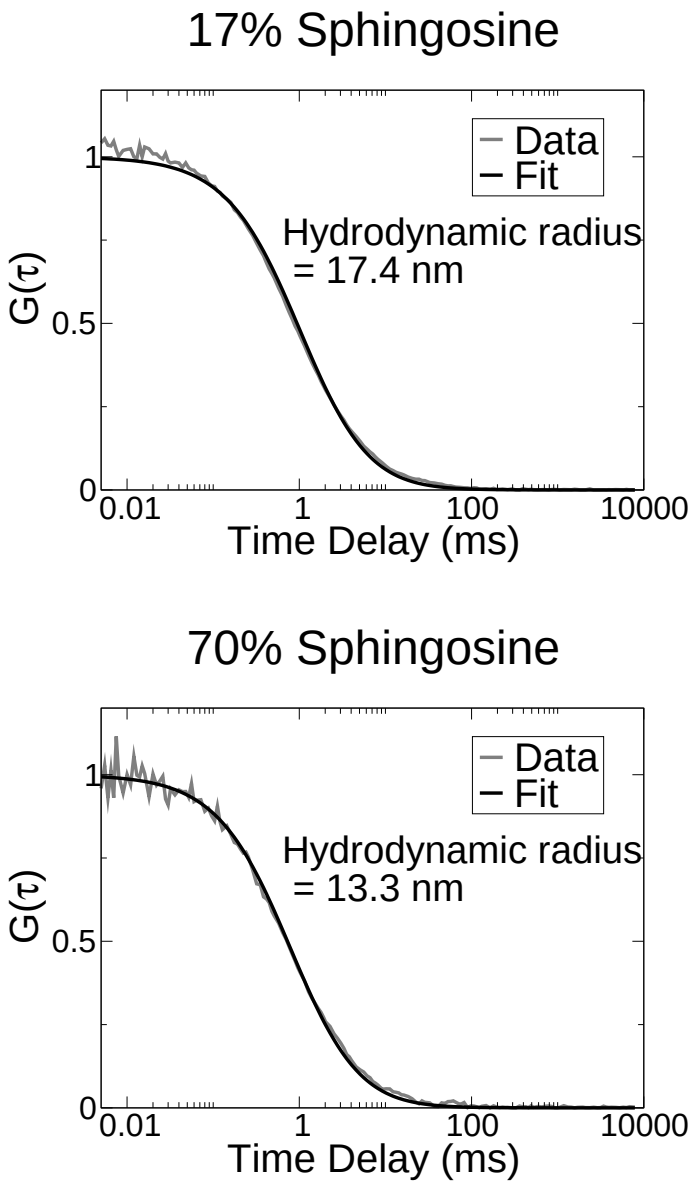

Figure 3.4: FCS curves of encapsulated dots. The fit to a single diffusion curve and the hydrodynamic radius imply that the dots are in single dot micelles, and are not aggregated.

quality of these dots are inferior to those produced by Dubertret and coworkers.

3.3 Sphingosine Phosphorylation Experiments

To test the dots for phosphorylation, the quantum dots were put in a fluorometer and their luminescence was monitored as enzyme and ATP were added. The enzyme and ATP were provided by Roisin Owens of David Russell's lab. The data are in Figure 3.5. While no shift in fluorescence was seen, the fluorescence intensity always decreased with ATP and the enzyme being added. Further tests showed that the fluorescence intensity only decreased when the enzyme was added whether or not ATP was added at all. The fluorescence was unchanged when just ATP was added to the dots. Also the fluorescence was decreased less for dots with a larger percentage of sphingosine on them and for dots with a smaller percentage of sphingosine on them. Therefore it seems as though the enzyme may be attaching to the sphingosine, this in turn causes the sphingosine to be more likely to go into solution and leave the dot. The quantum dot will lose fluorescence yield as it becomes unprotected.

3.4 Conclusion

After that point, experiments were stopped. It was decided that using the quantum dots in this way wasn't easy enough to continue. Russell's lab which provided the ATP and enzyme, had other methods to study the enzyme which were much more likely to produce results. While in the end the experiment didn't work, it was an interesting study in self-assembly of lipids around quantum dots. If one were to try again, serious consideration should be paid to trying to cross-link the

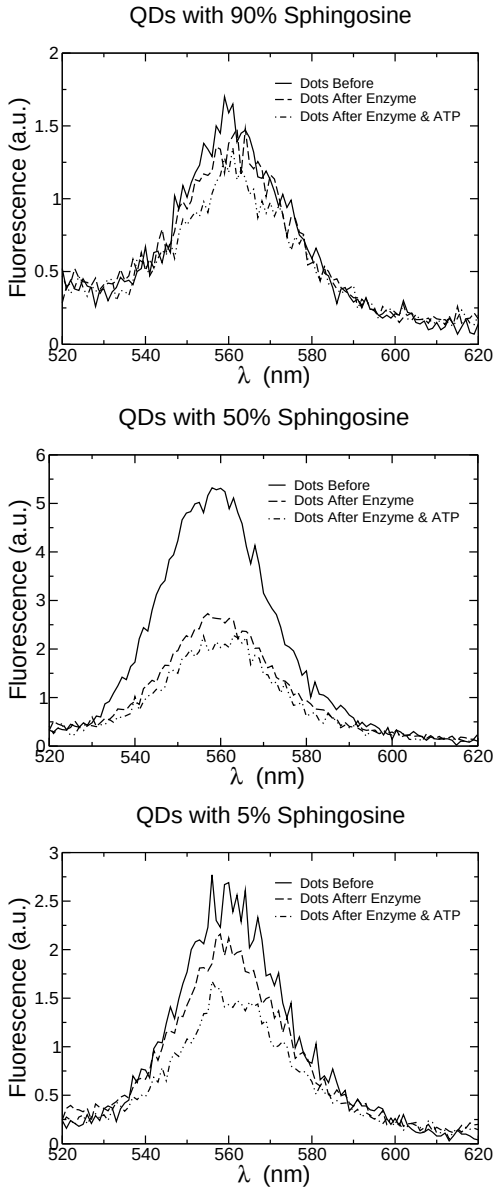

Figure 3.5: Data from the phosphorylation experiment. Top is data from dots with 90% sphingosine. Middle is data from dots with 50% sphingosine. Bottom is data from dots with 5% sphingosine.

lipids so that they don't come off the quantum dots. This will also improve the stability. There are many ways to attempt this. There are polymerizable lipids that upon exposure to ultraviolet light will cross-link[44]. There are also cross-linkable polymers that can be used, as was done for making carbon nanotubes water-soluble[45]. The overall mixture would not be fully biological, but that may not matter. Another avenue to pursue is the phosphorylation and dephosphorylation of other lipid systems. For instance there is an enzyme that removes the choline group from PC to make it PA. The issue of whether the quantum dots will feel the field of charges spread uniformly around its exterior, is another question that remains to be answered.

CHAPTER 4

CDSE/ZNS QUANTUM DOTS IN BIOLOGY, CONCLUSION

4.1 Revisiting the Membrane Potential Experiments

Due to the work encapsulating the quantum dots with sphingosine, not realizing the geometry considerations of the lipids while trying to get quantum dots into membranes was a mistake. Trying to make GUVs and BLMs with the dots in the lipid solution without altering the composition of the lipids will not work. The usual procedure to make both GUVs and BLMs require the long double chain lipids found in egg PC to make stable bilayers. To properly cover a quantum dot, lipids with a low critical packing parameter (CPP) are required. However, it is not clear that by altering the GUV or BLM lipid mixture with lower CPP lipids will allow GUVs or BLMs to form with quantum dots in them. Another structure may form instead. During the sphingosine experiments, when lipids with too large of a CPP were used, bilayers with quantum dots in them did not form. What appeared to be the encapsulation of two or more quantum dots in lipids seemed to be the result. It just may not be favorable for bilayers to self-assemble around a quantum dot.

However, if one prepared the bilayer system separately and the encapsulated quantum dot system separately, one might be able to get the quantum dots into the bilayer. To get the two together, an idea from drug delivery was borrowed. Cell membranes are usually negatively charged. There are rarely any naturally occuring positively charged lipids. A method in drug delivery is that a drug would be encapsulated in a vesicle that had positively charged lipids[46]. These vesicles would be attracted the cell membrane. They would bind and fuse together,

emptying the contents of the vesicle into the cell.

The goal then is to encapsulate the quantum dots in lipids, some of which have a positive charge. The DPPE-PEG/DPPC method was again not used, as the PEG may interfere with the quantum dot getting to the membrane. In fact water-soluble quantum dots from Quantum Dot Corporation were not used either. Those dots, along with most other published methods of making water-soluble dots, are made expressly to avoid sticking to membranes. They are meant to be attached to a specific molecule only.

It was not difficult to find a mixture of LMPC, EDLPC, and DLPC that would work. The EDLPC is a synthetic positively charged lipid. The actual method is cover in the appendix. It is interesting to note that the addition of a little (5 percent) sphingosine helped the encapsulation. Without it, there was a 4 nm redshift in fluorescence and a slight decrease in intensity. That seems to imply that the lipid mixture is not well optimized and that the sphingosine helps fill in gaps and lowers the CMC.

4.2 The *Aplysia* experiment

To test this idea, another voltage sensing experiment was tried. The system used was *Aplysia* neurons. Dan Dombeck of Webb group had this system setup, and was very familiar with it. It is described well in his paper[47]. An *Aplysia* neuron is voltage clamped, allowing the voltage across the membrane to be changed. The system has the sensitivity to detect 1% per 100 mV with averaging. The only modification of his experiment is the change in detection. His setup detected changes in second harmonic intensity versus voltage. As the quantum dots are expected to shift their fluorescence, not change their intensity, that setup wouldn't

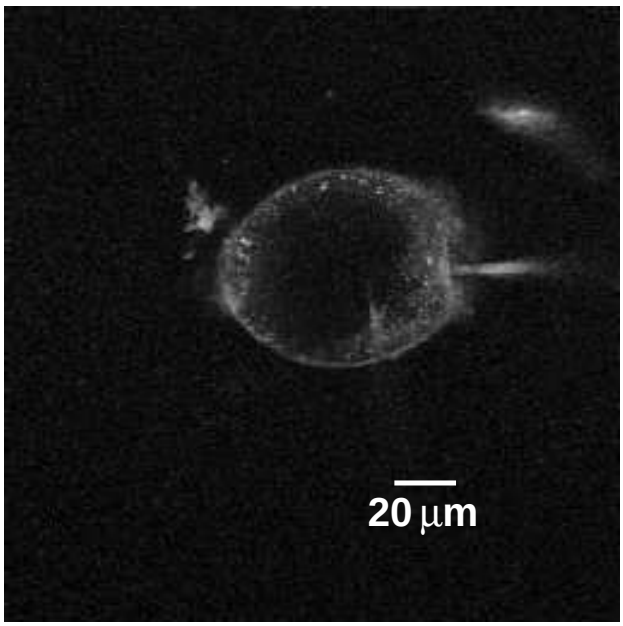

Figure 4.1: Picture of *Aplysia* labeled with quantum dots encapsulated with lipids.

work. Fortunately, his setup was easy to modify. The setup has two detectors. By splitting the collected fluorescence into the two detectors by means of a dichroic, a shift in fluorescence can be detected by a change in the ratio of the intensities of the detectors. Thus the dichroic converts a fluorescence shift into a intensity shift, which is what the setup usually measures. A dichroic was chosen that split the fluorescence in the center of spectrum.

Encapsulated quantum dots were prepared the day before the experiment. The dots were then introduced to the *Aplysia* neurons. No rinsing was performed. Usually a rinse or wash is performed after a fluorophore is added to cells, to remove any free fluorophore not attached. That was not needed, implying the dots all stuck to the membrane. Figure 4.1 is a picture taken of a *Aplysia* used for the measurement. One can see the clamp as it is the large straight piece coming from the cell.

While the fact that the quantum dots stuck to the membrane implied they were attracted to the membrane, the experiment overall was a failure. No fluorescence shift could be seen with voltage change. Worse still, the quantum dots seemed to lose flourescence intensity quickly, implying that they were not stable. It is also not certain that the dots were in the membrane, they may have just stuck to it. Electron microscopy would have to be done to confirm that. However, with Dombeck's work with second harmonic dyes to detect membrane potentials with this system working so well, there was little interest in diagnosing the problems and continuing the work.

4.3 Conclusion

CdSe/ZnS quantum dots are visible fluorophores with broad excitation and narrow emission. They also exhibit a Stark shift. The focus of this work was to exploit its Stark shift to observe biologically relevant processes. The quantum dots proved too difficult to work with in comparison to traditional methods. This fact is why it is difficult to imagine that CdSe/ZnS quantum dots will replace traditional fluorophores in general. Only in a few cases will they perform so significantly better that they will be worth the effort to get to work.

The property of broad excitation and narrow emission seems to be the most exploitable, as dyes are not and can not be made to have this property. Any experiment that requires multiple colors such as flow cytometry and multichannel FCS should benefit greatly from this[15]. The barcoding applications that also arise from this property will also be of great utility[48]. The applications that require multiple colors seem to be the future of CdSe/ZnS quantum dots, not applications that require its Stark effect.

If however, someone wished to continue this research there are some ideas to be pursued. For the sphingosine lipids, the cross-linking lipids or amphilic polymers should be investigated. Also using only core CdSe dots instead of core/shell CdSe/ZnS dots may prove to be more sensitive. As for the membrane measurements, the idea of first making the dots water soluble separately from the membrane system seems like the correct idea. With that in mind, it is probably wise to go back to the model membrane systems such as the black lipid membranes. The BLM system is quite robust and more importantly do not require growing cell cultures which take a significant amount of time. Cross-linking lipids for the membrane system may not work, but also could be investigated.

CHAPTER 5

NONLINEAR MEASUREMENTS OF PBSE QUANTUM DOTS

5.1 Introduction

The colloidal lead salt quantum dots are similar to the CdSe quantum dots in that they have broad excitation and narrow emission. They are different, however, in that they are strongly confined while the CdSe quantum dots are only intermediately confined. This is because the Bohr radius of both the electron and holes are quite large, 10 nm for PbS and 24 nm for PbSe[49].

While PbSe quantum dots have been made with a capping layer ($PbSe_xS_{1-x}$)[8], high quality lead salt quantum dots can be used without a capping layer similar to ZnS for the CdSe quantum dots. The other major difference is the wavelength of light at which they emit. The CdSe dots emit in the visible, while the lead salt quantum dots emit in the near infrared. This is because the band edge for CdSe is 730 nm while for PbS it is 3 μm and for PbSe it is 4.6 μm [9].

All but the smallest lead salt quantum dots are not useful in biology as water becomes highly absorptive in the near-infrared. The near-infrared is however, the wavelength range in which telecommunications are used. The major telecommunications bands are at 1550 nm and 1300 nm. There is a great desire to get good emitters, detectors, amplifiers, and optical switches in those wavelength ranges.

A general review of the electronic and optical properties of the lead salt quantum dots is given in Reference [50]. More detailed theoretical calculations of the lead salt quantum dots are given in References [51] and [52].

This study will concentrate on the third-order optical nonlinearity of the lead salt dots for the potential use of optical switching. Based on data from CdSe

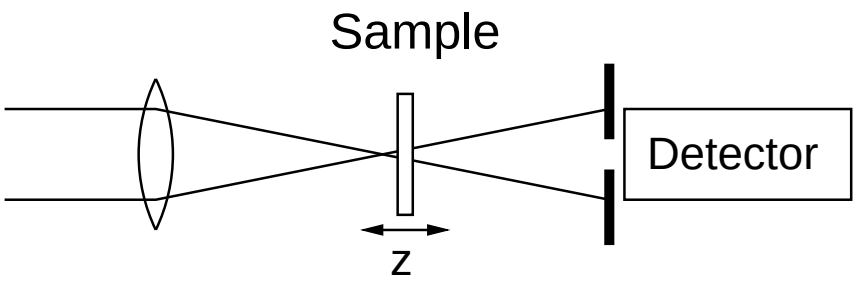

Figure 5.1: Diagram of the z-scan experiment.

quantum dots[53][54][55], we expect that the lead salt quantum dots will also have large a third-order optical nonlinearity. Also PbS quantum dots in glass have already been shown to have saturable absorption and have been used for that purpose in lasers[56][57][58][59]. The experiment we will use to measure the nonlinearity is the z-scan.

5.2 The Z-scan

The index of refraction on a third-order nonlinear material can be written as $n = n_0 + n_2 I$, where n_0 is the usual linear index of refraction and n_2 is the intensity dependent index of refraction representing the third-order nonlinearity. For reference, fused silica which makes the optical fibers that are the backbone of telecommunications has a $n_2 = 3 \times 10^{-16} \frac{cm^2}{W}$[60].

Because of the intensity dependence of the index of refraction, a beam with enough intensity will acquire a phase front that is proportional to the beam shape. Most beams are gaussian, and thus produce a gaussian phase front. This is very similar to the effect a lens has on a beam, though lens are spherical not gaussian usually. If n_2 is positive, the material acts as a focusing lens. If it is negative, the material acts a defocusing lens.

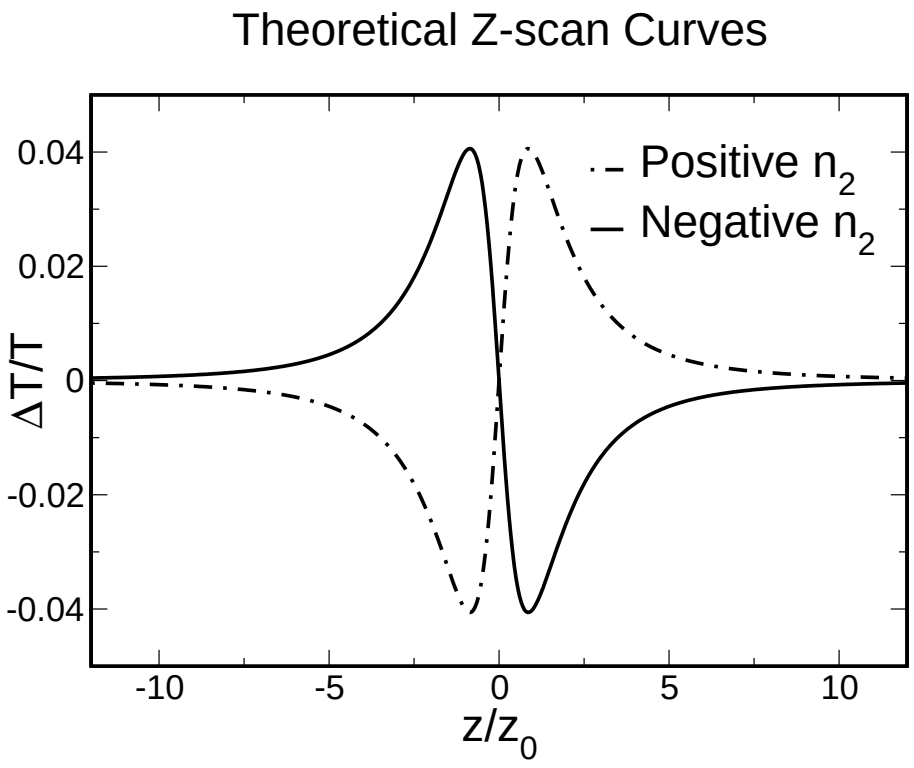

Figure 5.2: Theoretical z-scan curves for both a positive and negative n_2.

The z-scan experiment uses this property to determine n_2[61]. A diagram of a z-scan experiment is shown in Figure 5.1. It has a collimated beam incident on a focusing lens. The beam goes through the sample at a position z which is varied. After the sample there is a pinhole and a detector. When the sample is before the focus and n_2 is positive, the self-focusing of the sample will bring the overall focus of the beam towards the lens. This makes the beam at the pinhole larger, which lowers the detected intensity. After the focus the self-focusing property of the sample will make the beam at the pinhole smaller. This increases the detected intensity. The exact opposite of what was described happens if n_2 is negative.

Theoretical curves of the z-scan are shown in the Figure 5.2. The detected intensity which is also known as the intensity transmitted through the sample and

aperature is denoted as T. The plot shows the normalized change in transmitted intensity ($\Delta T/T$) versus the z position of the sample. The change, ΔT, is the difference between detected intensity when the sample is at the current position z and the detected intensity when it is at a position far from the focus. The horizontal axis of the plot is normalized to the confocal parameter of the focused beam, z_0.

The z-scan is not a very sensitive way to measure n_2. If the sample is non-uniform, as the sample moves and the beam hitting the sample changes size, the detected intensity will change without the nonlinearity just due to the non-uniformity. A more sensitive measurement is spectrally-resolved two-beam coupling[62]. This method works with femtosecond pulses when it is easy to resolve the spectrum of the laser. Picosecond and longer pulses do not have the bandwidth to easily spectrally-resolve energy shifts due to the nonlinearity. Long pulses were used in this study because of the concern that large bandwidth pulses would not be able to saturate the excited state of the quantum dots. The use of low peak power pulses also lowers the sensitivity of the experiment.

5.3 The Samples

The samples were provided by Evident Technologies of Troy, New York. They were provided in films sandwiched between two glass slides. The samples were usually labeled by their concentration before introduction to the host that comprised the film. Evident did not give specifics about how the films were made and what exactly the hosts were made of, so it is difficult to infer much about the quantum dots themselves. Several samples were given with different first exciton wavelengths. The most used samples were one with a first exciton wavelength at 1064 nm and

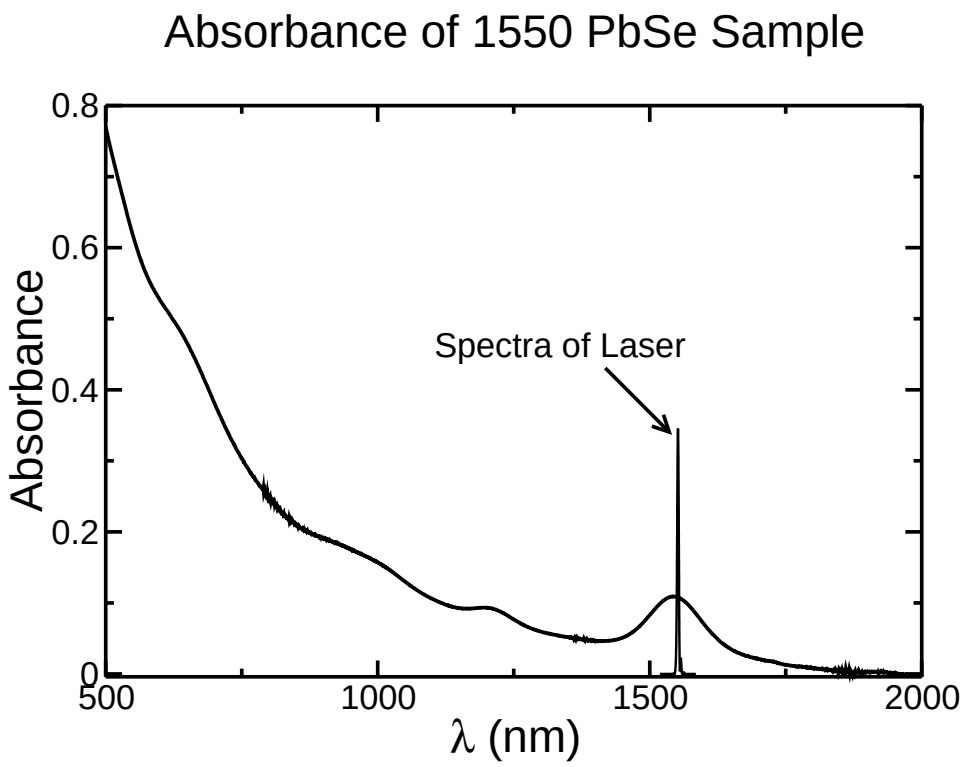

Figure 5.3: Absorption of 1550 nm sample and spectra of the laser used for the measurement.

another at 1550 nm. The quantum dots were put into films that were around 100 μm thick at an intial concentration of 100 mg/mL. The 1064 nm sample was used with a Nd:YAG Antares that was actively modelocked to produce 100 picosecond pulses with 200 nJ at 1064 nm. The 1550 nm sample was used with a Coherent Mira OPO system that produced 1 ps pulses with around 1 nJ of energy at 1550 nm. Both systems produce roughly the same order of magnitude peak power. Since the 1550 nm sample is at the more relevant wavelength, the rest of the chapter will deal with that sample. A plot with the absorption of the 1550 nm film and the spectra of the laser used to measure the sample is shown in Figure 5.3.

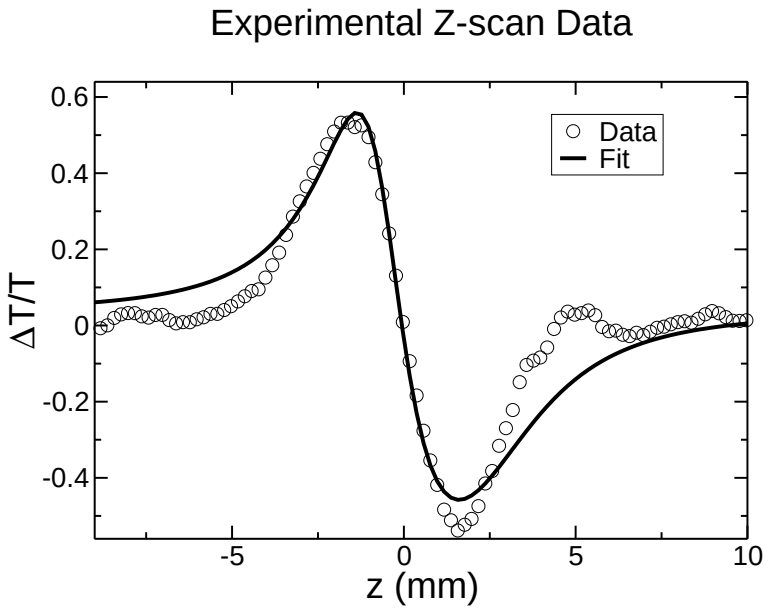

Figure 5.4: Sample z-scan data.

5.4 Experimental Results

A typical trace from the OPO experiment is shown in Figure 5.4. This shows a large negative nonlinearity. The data is fit using the equation from Reference [63] for large nonlinearities:

$$\Delta T/T = 1 - \left(1 - \frac{4x}{(1+x^2)^2}\Delta\Phi + \frac{4}{(1+x^2)^3}\Delta\Phi^2\right)^{-1} \tag{5.1}$$

The x in the equation is z/z_0. The confocal parameter, z_0, is estimated by measuring the beam width at several locations with a beam profiler and fitting for the beam width, w_0. The confocal parameter is related by the equation $z_0 = \frac{\pi w_0^2}{2\lambda}$. In this case the confocal parameter is about 1.8 mm which corresponds to a beam width of around 30 microns. The phase shift, $\Delta\Phi$, is equal to $\frac{2\pi}{\lambda}Ln_2I$, where I is the intensity and L is the thickness of the film. The fact that the curve doesn't fit well in the wings may be because of the two pieces of glass that sandwich the film

of quantum dots.

Unfortunately after careful analysis, this nonlinearity is due solely to thermal heating effects. Since the quantum dots absorb the laser light, some excess energy that is not emitted heats the sample. This causes a thermal gradiant that effects the index of refraction by changes in the density. This was first suspected when the repetition rate was reduced by an electro-optic modulator. Reducing the repetition rate reduces the average power incident on the sample by reducing the number of pulses hitting the sample, but does not change the peak power of the pulses. Reducing the repetition rate to 1 MHz from the usual 76 MHz caused the signal to disappear.

To further check the thermal nature of the z-scan result, a 30 hole chopper with all its holes covered but one and a boxcar were used to gate the signal. The boxcar was set to a 4 μs gate width and was scanned from when the chopper first let the pulses through (at 76 MHz repetion rate) to the time when the chopper closes. The beam was focussed with a 5 cm lens into the chopper to shorten the time it takes for the chopper to be fully open to the beam. The Figure 5.5 shows the peak of the signal versus the time when the chopper is open. This plot clearly shows a millisecond rise time indictative of a thermal nonlinearity. The thermal nonlinearity is not useful because of this long rise time. Telecommunications need fast (femtosecond) nonlinearities. While thermal nonlinearities have been studied[64][65], they give information about the host such as the heat conductivity and the change of index of refraction due to temperature. The thermal nonlinearity gives little about the quantum dots, as one would get the same effect from anything that produces an equivalent amount of heat. As Evident Technologies did not give much information on the host, there was little incentive to try to extract the host's qualities.

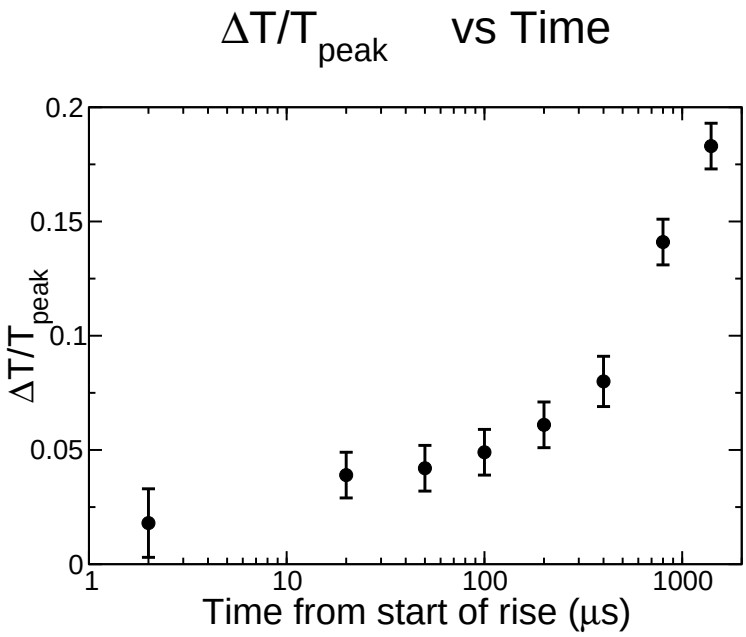

Figure 5.5: Data of the peak change of transmittance of the z-scan versus time from when the chopper opens and laser light is incident on the sample.

The existance of a large signal obscures the signal of interest, the nonlinearity from the electronic response. One way to mitigate this problem is to directly time-resolve the response of the nonlinearity using pump-probe techniques[66]. A diagram of the setup is in Figure 5.6. Here the beam is first split into two, a pump and a probe. The pump usually has 95% of the energy. The pump beam put through a half-wave plate to rotate the polarization by $\pi/2$ and into a variable time delay. Then it is recollimated with the probe beam and put into the z-scan setup. The sample is placed at a z position that should yield either a peak or a valley. The time delay between the pump and probe is then swept and the probe intensity is monitored. The pump beam is separated before the detector in the z-scan by a polarizing optic. An electronic nonlinearity will have a near instanteous rise time that should be clearly visible.

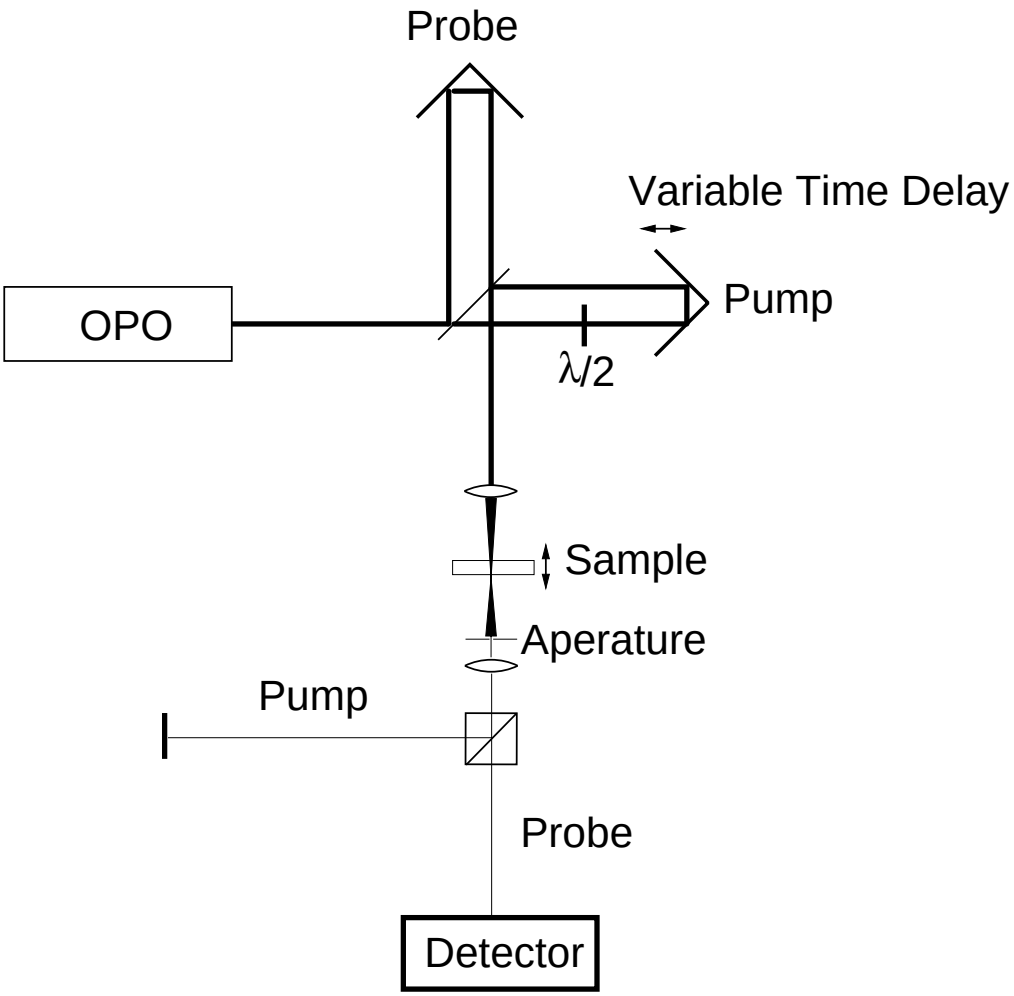

Figure 5.6: Diagram of the time resolved z-scan.

Unfortunately, no signal could be seen at the maximum light level capable from the OPO. An upper limit for the samples was put at 500 times the nonlinearity of fused silica. Current large nonresonant(fast) nonlinear materials are already available with this order of magnitude of nonlinearity [67].

5.5 Conclusion

Once the issue of the large nonlinearity due to thermal effects was taken into account, the electronic optical nonlinearity was too small to be measured. This means that lead salt quantum dots are not suitable for applications such as optical switching. A possible answer to why the nonlinearity is so small, will be discussed in the next chapter. In principle, one could try again with a picosecond optical parametric amplifier, which would have roughly 1000 times the peak power of the optical parametric oscillator. However, the isn't any access to one at Cornell.

CHAPTER 6

THE PHOTOLUMINSCENCE LIFETIME AND DIELECTRIC SCREENING OF PBS QUANTUM DOTS

6.1 Introduction

The lead salts are highly polarizable. The dielectric constant for PbS is 17 while for PbSe is 23. From Maxwell's equations, the field inside a sphere of dielectric constant ϵ_i is reduced from the field outside of dielectric constant ϵ_o by a factor $3\epsilon_o/(\epsilon_i + 2\epsilon_o)$. For the usual solvents such as cholorform which has a dielectric constant around 2, this can be a reduction factor of 4-5 for PbSe. If the field is reduced by that factor, then nonlinearities, which depend on the field to the 4th power, will be reduced accordingly. This could explain the small nonlinearity measured by the z-scan.

A way to check is to measure something that depends on the field and change the solvent. Guyot-Sionnest suggested that the dielectric screening effect is the reason why the quantum dots have longer lifetimes than theoretically expected [68]. This was also mentioned in the works of Schmitt-Rink[7] and Allen and Delerue[52]. Unlike the nonlinearity measurements, lifetime measurements are much simpler to do. A change of lifetime versus solvent has already been seen in the CdSe/ZnS quantum dots[69].

6.2 Lifetime Experiments

The lifetime of the PbS quantum dots were taken in a system originally put together from PicoQuant to do time-correlated single-photon counting. It amounts to a sample chamber that allows laser light to come in from one direction. The

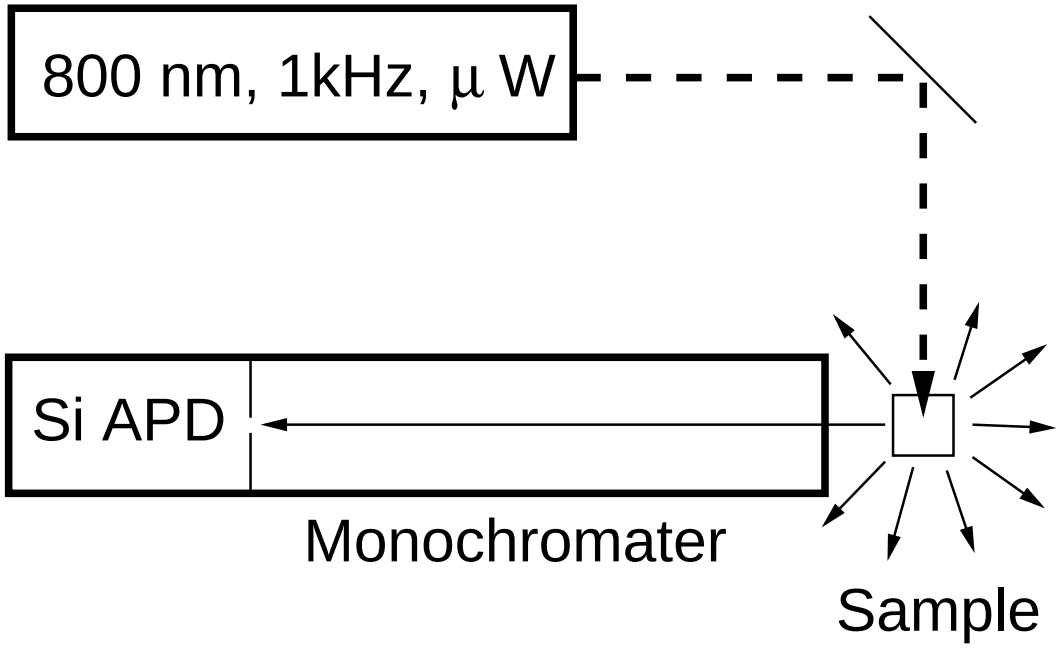

Figure 6.1: Diagram of the experimental setup used to measure fluorescent lifetimes.

luminescence is collected at a right angle to the beam. The luminescence is then put through a monochrometer into a detector. Figure 6.1 is a diagram of the experimental setup. Depending on the slit width, the monochromater could have wavelength resolutions of 8, 16 or 32 nm. The smaller 0.5 mm slits were used in most cases which gave the monochromater 8 nm resolution.

The excitation was a Clark MXR regenerative amplifier capable of producing 400 μJ pulses at 800 nm at a 1 kHz repetition rate (400 mW average power). This laser was used mainly because it had a low repetition rate which allowed the sample to fully relax between pulses. The sample was only exposed to μW average power levels so that the sample was always kept below one excitation per quantum dot.

Detectors, especially single photon counters, have always been difficult to obtain

in the near infrared. They are usually plagued by noise and large dark counts. A germanium avalanche photodiode (Ge APD) came with the PicoQuant system, but had far too many dark counts, 10^3 counts/s. The best detector in the near infrared is a silicon single photon counting APD. A Perkin-Elmer single photon counting APD was attached to the lifetime setup. It has only 40 dark counts per second. The output was then fed into a SRS430 multichannel scalar. Both the detector and SRS430 were borrowed from Webb group. The silicon detector only can detect out to 1100 nm in theory, but as it has very low dark counts it can detect out to 1150 nm and still have better performance than the Ge APD. Fortunately, PbS quantum dots that emit below 1100 nm are commercially available. The SRS430 had minimum time resolution of 5 ns, which while large is much smaller than the measured lifetimes. While it would be preferable to measure the PbSe quantum dots used in the previous chapter, the PbS quantum dots are similar enough that the conclusion drawn should apply to the PbSe quantum dots.

Two different samples purchased from Evident Technologies roughly 2 months apart. They were both PbS quantum dots with first exciton peak at 770 nm and center of emission at 920 nm. They were dispersed in either tetrachloroethylene (TCE), chloroform, or hexane. TCE has an index of refraction of 1.50, while hexane has an index of refraction of 1.38. Chloroform is in the middle with an index of refraction of 1.44. None of the solvents have absorption resonances at 920 nm. Since TCE has the least contrast in dielectric constant with PbS, it is expected to have the shortest lifetime. Hexane should have the longest lifetime.

The data from the two different samples is shown in Figure 6.2. The data are fitted to a single exponential function, $A\exp(-t/\tau_L)$, where τ_L is the lifetime. The data fitting is weighted to the square root of the counts. This is the expected

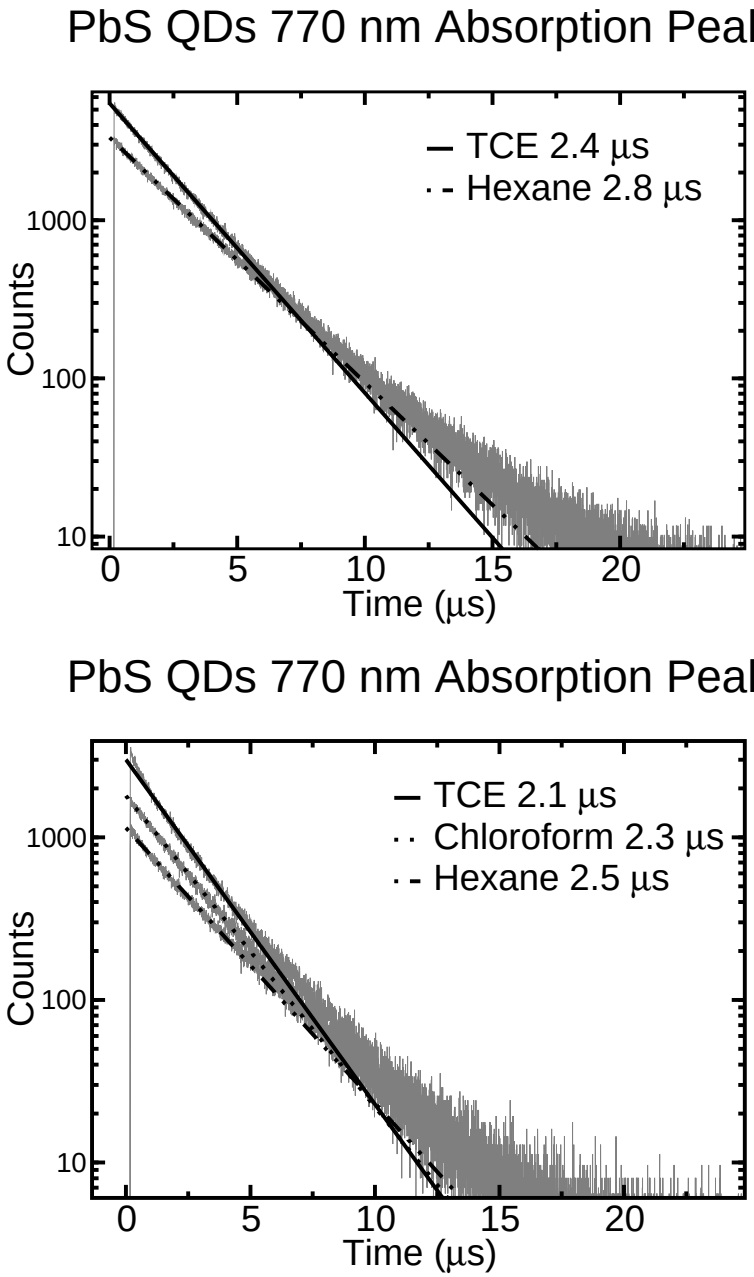

Figure 6.2: Data showing the variation of lifetime versus solvent.

error for a Poisson process. The data near the top of the curve is considered more accurate than the data near the bottom and the fitting uses this. Also data with less than around 10 to 100 counts were neglected in the fitting. The data with low photon counts is suspect because of the influence of dark counts from the detector.

The lifetimes are offset, but clearly show that the lifetime of the quantum dots in TCE is indeed shorter than that from chloroform or hexane. However, using the simple classical model of dielectric screening, the quantum dots in hexane should have 30% longer lifetime than that of the TCE. The actual result is just below 20%. This could because the index of refraction given is not at the correct wavelength. Also the classical model may not apply exactly to quantum dot systems. The work with the CdSe/ZnS quantum dots implied a nonclassical dielectric screening[69]. The models put forward in that paper though neglect the dielectric constant of the CdSe, and also would give a much smaller variation with respect to index of refraction than is observed in this experiment with the PbS quantum dots[69]. While both samples show the approximately correct dielectric screening, they do not have consistent lifetimes. This indicates that quantum dots are not being synthesized consistently as of yet. Nonetheless, for these dots the lifetime can be said to be approximately 2 μs long. This is relatively consistent with earlier measurements on colloidal PbS quantum dots which measured 1 μs lifetimes[70].

6.3 Fluorescence Resonant Energy Transfer

When the PbS quantum dots that were studied are dried into a close packed film, the luminescence red shifts from 920 nm by roughly 40 nm to 960 nm, as in Figure 6.3. It is believed that fluorescence (or Förster) resonant energy transfer (FRET) is responsible for the shift. FRET uses the long range dipole-dipole interaction

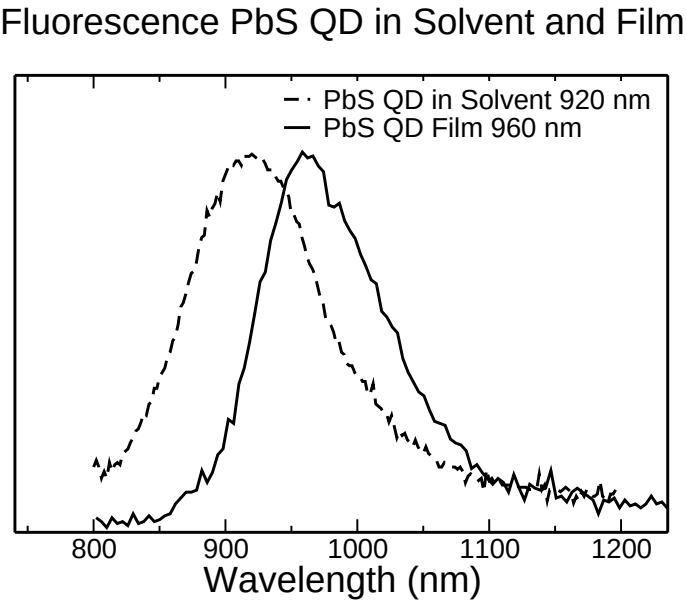

Figure 6.3: Fluoresence shift in a film of quantum dots.

to effectively transfer energy between a fluorophore to another one with a lower energy state *without* emission and reabsorption. Since any sample of quantum dots always has distribution of sizes, the energy transfer is between slightly smaller dots to slightly larger dots.

FRET has be studied extensively in the CdSe quantum dots[71][72][73]. Biosensors based on FRET have been demonstrated[74]. FRET has also been demonstarted as a way to pump CdSe quantum dots for light emitting devices[75][76][77]. The ability to transfer energy into and out of quantum dots nonradiatively has proven to be very useful in the CdSe quantum dots, and may also be in the lead salt quantum dots.

By spectrally resolving the fluorescence from the quantum dot films, energy transfer can be confirmed. The films were created by first putting the PbS quantum dots in chloroform. Then the dots in chloroform where put onto a glass coverslip

and the chloroform was allowed to evaporate. The data shown in the Figure 6.4 shows the lifetime at different wavelengths. The data clearly shows energy transfer from the high energy to the low energy wavelengths on a time scale of roughly 200 ns.

FRET is usually done between two distinct fluorophores as was done in Reference [78][79][80]. The fact that FRET is happening in a distribution of fluorophores greatly complicates the analysis. A quantum dot can be both a donor and an acceptor. From the data at 920 nm (the center the emission of the solution) the emitting dot is apparently is neither a net donor or acceptor. Nonetheless if the single dot absorption and emission linewidths are known then a numerical analysis of the data can be performed similar to the work done by Kagan and coworkers[72]. However, the single dot linewidths are not known well. Since the PbS data match similar data for the CdSe quantum dots from Kagan and coworkers and other research groups[72][73], the 40 nm luminescence shift and the 200 ns FRET transfer time will be sufficient to describe this measurement.

In the interest of being able to calculate a Förster radius, an experiment between two "distinct" sizes of quantum dots was performed similar to that done by Kagan and coworkers[72]. While both samples will have a size distribution, they will be approximated as two distinct fluorophores. PbS quantum dots with first exciton peak at 770 nm and emission centered at 920 nm were mixed with PbS quantum dots with first exciton peak at 880 nm and emission centered at 1012 nm. The overlap between the emission of the 770 nm quantum dots and the absorption of the 880 nm quantum dots is shown in Figure 6.5.

The emission of the dots mixed in solvent (TCE) and dried on the film are shown in Figure 6.6. While in the solvent the emission of the combined dots shows

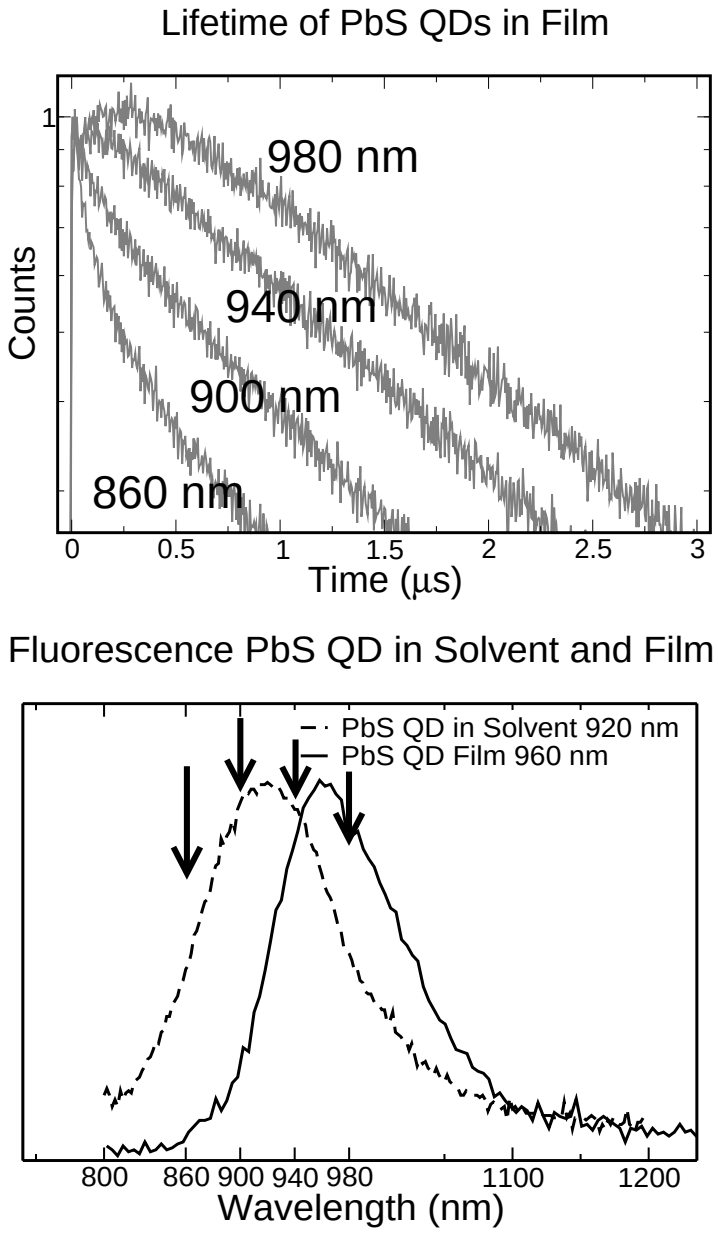

Figure 6.4: Spectrally and time resolved fluorescence of the quantum dot film.

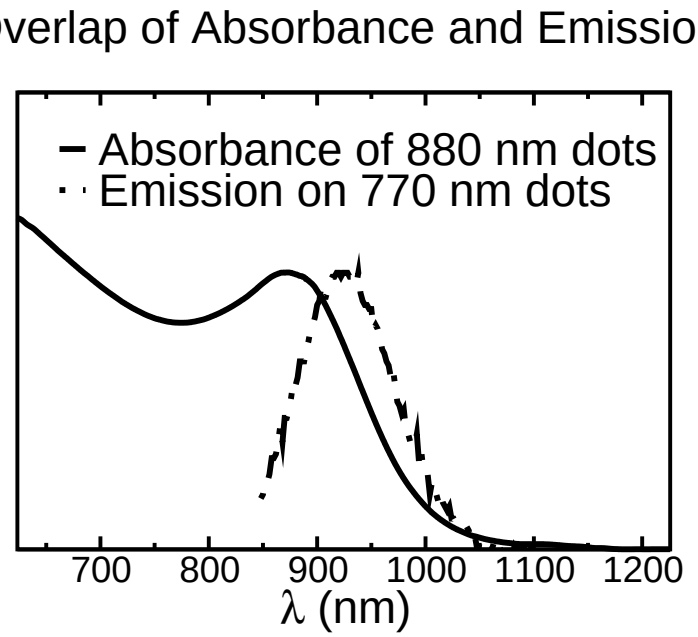

Figure 6.5: Overlap of the emission from the 770 nm qauntum dots with the absorbance of the 880 nm quantum dots.

a superposition of the individual emission spectra, the dots dried in film show emission that looks similar to the emission of the 880 nm dots only. The shift in luminescence is from 950 nm in solution by 100 nm to 1050 nm.

To calculate a Förster radius, R_0, the formula as followed is used[81].

$$R_0^6 = \frac{9000\kappa^2 \ln 10}{128\pi^6 n^4 N_{AV}} \Phi_d \int_0^\infty E_d(\nu)\epsilon_a(\nu)\frac{d\nu}{\nu^4} \tag{6.1}$$

κ^2 is an orientation factor that is assigned 2/3. N_{AV} is Avogadro's number. Φ_d is the quantum yield of the donor. $E_d(\nu)$ is the normalized donor emission spectra. $\epsilon_a(\nu)$ is the molar extinction coefficient of the acceptor. There some uncertainity in some of these numbers. The concentration is not known but is estimated from the size of the quantum dots and the known mass of lead salt per mL. This gives an estimated ϵ_a at the first exciton peak of $8 \times 10^4 M^{-1} cm^{-1}$. The quantum yield is taken to be around 50 % but it is not known. Given data from Reference [68], 50%

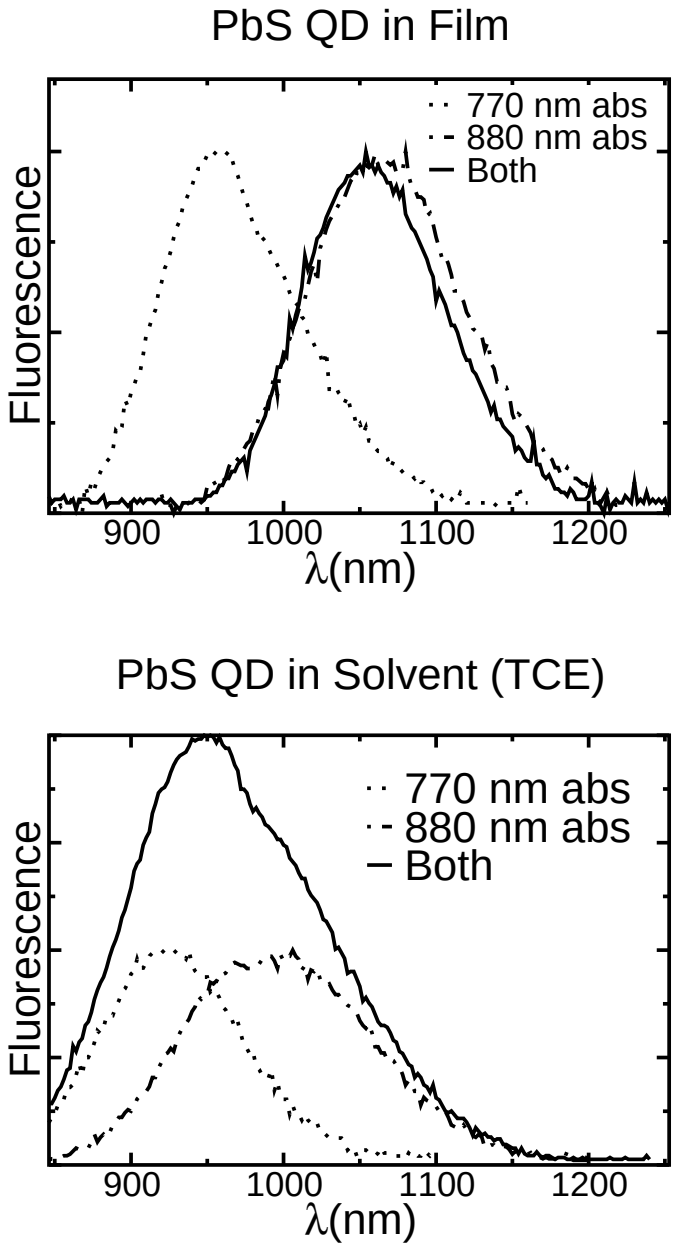

Figure 6.6: Fluorescence of the combination of dots in solvent (top) and in a film (bottom).

is not unreasonable. The quantum yield is not easily measured for a fluorophore in the near infrared. The overlap integral is calculated with the absorption and emission from Figure 6.5 with the assumption that there are only two fluorophores. The actual integral should be over the single particle absorption and emission. This calculation is only to get a rough idea of the Förster radius. With all the numbers put into the equation a Förster radius of 80Å is calculated. Note due to the sixth power in the exponent, a 50% error in the calculation is only a 7Å error in the radius. The calculated Förster radius is within an order of magnitude of a reasonable number.

Spectrally resolving the fluorescence again shows the energy tranfer. The data is shown in Figure 6.7. The transfer time appears to be between 200 and 400 ns. The theoretical transfer time is given by the equation:

$$\tau = \tau_d \left(\frac{R}{R_0} \right)^6 \tag{6.2}$$

In the equation τ_d is the lifetime of the donor taken to be 2.5 μs. This gives a separation distance between 50 and 60 Å. Even though the estimate is quite rough, it gives a distance that is quite plausible for a close packed quantum dot film.

Another way to look at the previous experiment is to think of the two dots together not as two dots, but as one sample of dots with a large size distribution. The much larger spectral shift fits well with the calculated work done by Kagan and coworkers[72]. A larger size distribution leads to a larger spectral shift.

6.4 Conclusion

The PbS quantum dots have long lifetimes, around 2 μs. Dielectric screening can explain this fact, and dielectric screening can also help explain the lack of a

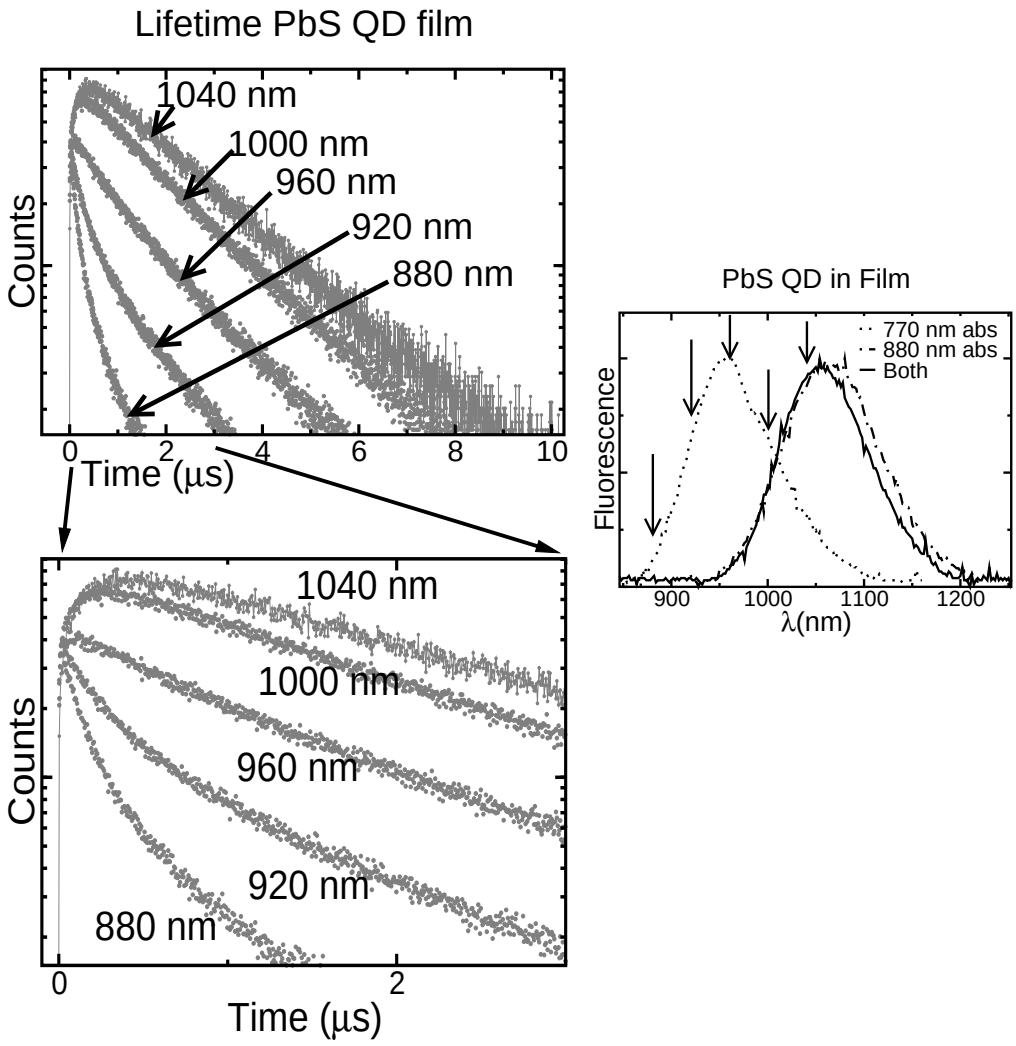

Figure 6.7: Spectrally and time resolved fluorescence of the quantum dot film.

nonlinear signal measured. The PbS quantum dots exhibit FRET very similar to the CdSe quantum dots. The FRET times are longer because the lifetimes are longer. If more were known about the intrinsic properties of the PbS, then a more detailed analysis similar to Kagan and coworkers[72] could be performed. It would also be beneficial if the lifetime of the dots in solvent were consistent between samples produced at different times.

While it is important to verify that FRET takes place in PbS films and that it is the cause of the luminescence shift, the there is no novelty in the observation because it so closely mirrors the work done with the CdSe quantum dots. The really interesting work is to use FRET to transfer energy into the quantum dots from other sources similar to the work done by Klimov's group [75][76] and by Anni and coworkers[77]. Questions such how does dielectric screening affect the transfer times, and what effect does the large difference in lifetimes between donor and acceptor mean for applications, will have to be answered.

While the lead salt quantum dots do not look favorable as nonlinear materials, the future of the lead salt quantum dots looks quite promising. Recent research by other groups such as impact ionization in the lead salts that may lead to more efficient solar cells will help keep the field strong for several more years[82].

APPENDIX A

METHODS FOR ENCAPSULATING QUANTUM DOTS IN LIPIDS

A.1 Introduction

The encapsulating procedure is based roughly on the work of Dubertret and coworkers [14]. It involves three main steps. Washing is performed to get rid of excess ligand. Then the actual encapsulation step is next. Then a filtering step is performed last of all.

Unless otherwise noted, all lipids came from Avanti Polar Lipids of Alabaster, Alabama. The quantum dots were donated by Professor Todd Krauss of Rochester University. Care must be taken in using this synthesis with dots from other sources. Coworkers in the Wise group lab, Byung-Ryool Hyun and Sareet Jacob[83], found that to encapsulate quantum dots from Evident Technologies, ligand exchange had to be performed.

A.2 Washing the Dots

Washing the dots is actually a method to remove the excess ligand, which is usually trioctylphosphine oxide (TOPO), from solution. The dots are grown in a solution that is rich in TOPO and they are usually stored and shipped in solution with excess TOPO. The excess TOPO in the solution helps keep the dots stable over several months. Therefore one should wash the dots only before they plan to encapsulate them. Washed dots last at least a few weeks.

If the excess TOPO is not removed from the solution, the dots will not be encapsulated. TOPO is very hydrophobic, and if there is excess, the lipids will form micelles around the free TOPO and not the quantum dots. The result is

a foamy solution of TOPO-lipid micelles and quantum dot aggregates. However, washing the dots also can damage them. If the dots are washed too often, too much TOPO will be removed from the dots. Then the dots will precipitate out of the nonpolar organic solvents. The dots without the TOPO aren't hydrophobic enough, and won't form a micelle. The water will then destroy them. Depending on the source of quantum dots, one may have to wash the dots slightly differently as different sources may have differing amounts of ligand with the quantum dots.

The basic concept of washing is that the dots are put into a slightly polar solvent, methanol. Then the dots are centrifuged. The dots end up on the bottom of the centrifuge tube and excess TOPO is left in solution which is then removed. The precipitated quantum dots are then reintroduced to a nonpolar organic solvent. If they haven't been washed too many times, they will go back into solution. A little experimentation may be required to get the washing correct when dealing with a new source of quantum dots.

The quantum dots came from Professor Krauss in hexane at 15 μM. The dot to slightly polar solvent ratio used in washing was 1 to 3. Since a microcentrifuge that held 1.5 mL eppendorf tubes was used to precipitate the quantum dots, 700 μL of dots were washed at a time. 350 μL of dots was mixed with 997.5 μL methanol and 52.5 μL of butanol and put into a tube. On the advise of Professor Krauss a small amount of butanol was used. Methanol by itself seemed to work fine as well though. The 1.4 mL of solution was put into two 1.5 mL eppendorf tubes. The two tubes were put into the centrifuge opposite each other for balance. The centrifuge was then run at 10,000 rpm for 5 minutes. After that, the dots were at the bottom of the eppendorf tube. The solution was poured off, and 350 μL of hexane was put into the tube. After a slight shake the quantum dots went back

into solution. This step was performed three times and then the dots were stored in a glass vial until they were used.

A.3 Encapsulating the Dots

Encapsulating the dots is quite straightforward. Washed dots were mixed with the lipids which were in chloroform in a glass vial or test tube. The lipid to dot ratio was around 2000 to 1. Then excess chloroform was added to the mixture. The reason for the extra chloroform is that the dot lipid mixture when evaporated must form a thin film on the glass. If the film is thick, the dots will be aggregated when the water is added and usually stay that way. Typical numbers were 25 μL of dots with 400 μL of excess chloroform plus whatever chloroform came with the lipids. The actual amount of extra chloroform added depends on the glass tube used. The extra 400 μL is for a 4 mL glass vial. If a different glass tube or vial is used, the extra chloroform needed may have to be adjusted.

The mixture is evaporated under nitrogen in a fume hood. Then clean water at room temperature is added and the mixture is covered. The mixture is allowed to sit at room temperature overnight. Temperature is expected to play a part in the self-assembly of the lipid-dot micelles, but experimentally temperature didn't seem to matter much. It is worth more investigation though. The next day the mixture was quickly, less than 30 seconds, ultrasonicated. Too much sonication will also kill the dots. Then the dots are ready to be filtered.

A table of lipid combinations that worked is listed in Table A.1. The first column is the amount of single chain lipid used. LMPC has a single 14 unit fully saturated hydrocarbon chain with the phosphatidylcholine head group. The second column is the double chain lipid used. DMPC has a double chain 14 units long

Table A.1: Table of the different combinations of lipids that produced single quantum dot micelles.

5 % LMPC		5 % EDMPC	90 % SS
40 % LMPC	5 % DMPC	5 % EDMPC	50 % SS
50 % LMPC	40 % DMPC	5 % EDMPC	5 % SS
33 % LMPC	33 % DMPC	17 % EDMPC	17 % SS
50 % LMPC			50 % SS
40 % LMPC	40 % DLPC	20 % EDLPC	
50 % LMPC	40 % DLPC	10 % DLPA	
20 % LMPC		10 % EDLPC	70 % SS

and DLPC has a double chain 12 units long. Both have fully saturated hydrocarbon chains and have the phosphatidylcholine head group. The third column is the charged lipid used. EDMPC and EDLPC are like DMPC and DLPC respectively except the head group is ethylphosphatidylcholine. Ethylphosphatidylcholine has the phosphate group neuralized so it is a positively charged head group. DLPA is a 12 unit fully saturated double hydrocarbon chain lipid with the phosphatic acid head group which is negatively charged. SS stands for sphingosine. The phosphatidylcholine lipids were used mainly because they are inexpensive compared with lipids with other head groups.

A.4 Filtering the Dots

Although it is possible to have the lipids just right to encapsulate all the dots into single dot micelles, often there will be a small percentage that form two or

more dots per micelle. In order to get rid of the non-single dot micelles, filtering is performed. Syringe filters from Millipore were used. The membrane filters that fit into the syringe are disposable and the syringe is reusable. Two filters were used from Millipore, one with 220 nm pore and the other with a 25 nm pore. Unless the method of encapsulating is known to produce mostly single QD micelles, the 220 nm pore filter is used first. This gets rid of any large aggregates that may clog the smaller filter. Also these are 60% cheaper than the 25 nm pore filters. If the quantum dots don't go through this filter or are very difficult to go through this filter, then the lipid mixture won't work. The smaller filter is then used. If a substantial number of quantum dots go through the filter (and this is checked by a fluorometer or a UV lamp), then the encapsulation procedure worked.

Fluorescence correlation spectroscopy was performed both before and after the filtering on many samples. Only a few samples could have simple diffusion fits without filtering. Most encapsulation procedures that worked often would have one or two quantum dot aggregrates go through the diffusion volume in the five minutes it took to take data. Only one aggregate is enough to alter the FCS curve. With filtering, the encapsulated quantum dots produce clean FCS curves.

BIBLIOGRAPHY

[1] C. B. Murray, D. J. Norris, and M. G. Bawendi, J. Am. Chem. Soc. **115**, 8706 (1993).

[2] C. B. Murray, S. H. Sun, W. Gaschler, et al., IBM J. Res.Dev. **45**, 47 (2001).

[3] S. Kim and M. G. Bawendi, J. Am. Chem. Soc. **125**, 14652 (2003).

[4] H. Mattoussi, J. M. Mauro, E. R. Goldman, G. P. Anderson, V. C. Sundar, F. V. Mikulec, and M. G. Bawendi, J. Am. Chem. Soc. **122**, 12142 (2000).

[5] A. L. Efros and A. L. Efros, Sov. Phys. Semicond. **16**, 772 (1982).

[6] L. E. Brus, J. Chem. Phys. **80**, 4403 (1984).

[7] S. Schmitt-Rink, D. A. B. Miller, and D. S. Chemla, Phys. Rev. B **35**, 8113 (1987).

[8] M. Brumer, A. Kigel, L. Amirav, A. Sashchiuk, O. Solomesch, N. Tessler, and E. Lifshitz, Adv. Funct. Mater. **15**, 1111 (2005).

[9] S. M. Sze, *Physics of Semiconductor Devices* (Wiley, New York, 1981).

[10] M. A. Hines and P. Guyot-Sionnest, J. Phys. Chem. **100**, 468 (1996).

[11] X. Peng, J. Wickham, and A. P. Alivisatos, J. Am. Chem. Soc. **120**, 5343 (1998).

[12] M. Bruchez Jr., M. Moronne, P. Gin, S. Weiss, and A. P. Alivisatos, Science **281**, 2013 (1998).

[13] W. C. W. Chan and S. Nie, Science **281**, 2016 (1998).

[14] B. Dubertret, P. Skourides, D. J. Norris, V. Noireaux, A. H. Brrivanlou, and A. Libchaber, Science **298**, 1759 (2002).

[15] W. C. W. Chan, D. J. Maxwell, X. Gao, R. E. Bailey, M. Han, and S. Nie, Curr. Opin. Biotechnol. **13**, 40 (2002).

[16] V. L. Colvin and A. P. Alivisatos, J. Chem. Phys. **97**, 730 (1992).

[17] V. L. Colvin, K. L. Cunningham, and A. P. Alivisatos, J. Chem. Phys. **101**, 7122 (1994).

[18] V. L. Colvin, Ph.D. thesis, University of California at Berkeley, 1994.

[19] S. A. Empedocles and M. G. Bawendi, Science **278**, 2114 (1997).

[20] X. Wu, H. Liu, J. Liu, K. N. Haley, J. A. Treadway, J. P. Larson, N. Ge, F. Peale, and M. P. Bruchez, Nature Biotechnol. **21**, 41 (2003).

[21] M. Nirmal, B. O. Dabbousi, M. G. Bawendi, J. J. Macklin, J. K. Trautman, T. D. Harris, and L. E. Brus, Nature **383**, 802 (1996).

[22] D. R. Larson, W. R. Zipfel, R. M. Williams, S. W. Clark, M. P. Bruchez, F. W. Wise, and W. W. Webb, Science **300**, 1434 (2003).

[23] D. R. Larson, Ph.D. thesis, Cornell University, 2004.

[24] W. W. Webb, Appl. Opt. **40**, 3969 (2001).

[25] H. Mattoussi, A. W. Cumming, C. B. Murray, M. G. Bawendi, and R. Ober, Phys. Rev. B **58**, 7850 (1998).

[26] M. Pelton, D. G. Grier, and P. Guyot-Sionnest, Appl. Phys. Lett. **85**, 819 (2004).

[27] M. Kuno, D. P. Fromm, H. F. Hamann, A. Gallagher, and D. J. Nesbitt, J. Chem. Phys. **112**, 3117 (2000).

[28] T. J. Rink, C. Montecucco, T. R. Hesketh, and R. Y. Tsien, Biochim. Biophys. Acta **595**, 15 (1980).

[29] E. F. Fluhler, V. G. Burnham, and L. M. Loew, Biochemistry **24**, 5749 (1985).

[30] H. T. Tien, *Bilayer Lipid Membranes (BLM): Theory and Practice* (Dekker, New York, 1974).

[31] L. Moreaux, T. Pons, V. Dambrin, M. Blanchard-Desce, and J. Mertz, Opt. Lett. **28**, 625 (2003).

[32] L. Mathivet, S. Cribier, and P. E. Devaux, Biophys. J. **70**, 1112 (1996).

[33] K.-i. Akashi, H. Miyata, H. Itoh, and K. Kinosita Jr., Biophys. J. **71**, 3242 (1996).

[34] T. J. Rink, C. Montecucco, T. R. Hesketh, and R. Y. Tsien, Biochim. Biophys. Acta **595**, 15 (1980).

[35] C. Bronner and Y. Landry, Biochim. Biophys. Acta **1070**, 3321 (1991).

[36] A. H. Merill, Jr., E-M. Schmelz, D. L. Dillehay, S. Spiegel, J. A. Shayman, J. J. Schroeder, R. T. Riley, K. A. Voss, and E. Wang, Toxicology and Applied Pharmacology **142**, 208 (1997).

[37] J. N. Israelachvili, *Intermolecular and Surface Forces* (Academic Press, Orlando, 1985), pp. 229-275.

[38] K. Holmberg, B. Jönsson, B. Kronberg, and B. Lindman, *Surfactants and Polymers in Aqueous Solution* (John Wiley & Sons, Ltd, West Sussex, England, 2003).

[39] C. Tanford, *The Hydrophobic Effect: Formation of Micelles and Biological Membranes* (Wiley, New York 1980).

[40] D. Marsh, *CRC Handbook of Lipid Bilayers* (CRC Press, Boca Raton, FL, 1990), p. 276-279.

[41] K. Sou, T. Endo, S. Takeoka, and E. Tsuchida, Bioconjugate Chem. **11**, 372 (2000).

[42] H. Heerklotz and R. M. Epand, Biophys. J. **80**, 271 (2001).

[43] J. Eastoe and J. S. Dalton, Langmuir **14**, 5719 (1998).

[44] D. S. Johnston, S. Sanghera, M. Pons, and D. Chapman, Biochim. Biophys. Acta **602**, 57 (1980).

[45] Y. Kang and T. A. Taton, J. Am. Chem. Soc. **125**, 5650 (2003).

[46] R. C. MacDonald, G. W. Ashley, M. M. Shida, V. A. Rakhmanova, Y. S. Tarahovsky, D. P. Pantazatos, M. T. Kennedy, E. V. Pozharski, K. A. Baker, R. D. Jones, H. S. Rosenzweig, K. L. Choi, R. Qui, and T. J. McIntosh, Biophys. J. **77**, 2612 (1999).

[47] D. A. Dombeck, M. B.-Desce, and W. W. Webb, J. Neurosci. **24**, 999 (2004).

[48] M. Han, X. Gao, J. Z. Su, and S. Nie, Nature Biotechnol. **19**, 631 (2001).

[49] *Landolt-Bornstein: Numerical Data and Functional Relationships in Science and Technology, New Series* edited by O. Madelung, M. Schultz, and H. Weiss (Springer-Verlag, 1982).

[50] F. W. Wise, Acc. Chem. Res. **33**, 773 (2000).

[51] I. Kang and F. W. Wise, J. Opt. Soc. Am. B **14**, 1632 (1997).

[52] G. Allan and C. Delerue, Phys. Rev. B **70**, 245321 (2004).

[53] L. E. Brus, Appl. Phys. A **53**, 465 (1991).

[54] V. Klimov in *Handbook on Nanostructured Materials and Nanotechnology*, H. Nalwa, ed., (Academic Press, San Diego, CA, 1999) Volume 4, p 451.

[55] M. Yamane and Y. Asahara, *Glasses for Photonics* (Cambridge University Press, Cambridge, United Kingdom, 2000).

[56] P. T. Guerreiro, S. Ten, N. F. Borrelli, J. Butty, G. E. Jabbour, and N. Peyghambarian, Appl. Phys. Lett. **71**, 1595 (1997).

[57] K. Wundke, S. Pötting, J. Auxier, A. Schülzgen, N. Peyghambarian, and N. F. Borelli, Appl. Phys. Lett. **76**, 10 (2000).

[58] J. F. Philipps, T. Töpfer, H. Ebendorff-Heidepriem, D. Ehrt, R. Sauerbrey, and N. F. Borrelli, Appl. Phys. B **72** 175 (2001).

[59] A. M. Malyarevich, V. G. Savitski, P. V. Prokoshin, N. N. Posnov, K. V. Yumashev, E. Raaben, and A. A. Zhilin, J. Opt. Soc. Am. B **19** 28 (2002).

[60] G. P. Agrawal, *Nonlinear Fiber Optics* (Academic Press, San Diego, California 1995) p 583.

[61] M. Sheik-Bahae, A. A. Said, T.-H. Wei, D. J. Hagan, and E. W. Van Stryland, IEEE J. Quantum Electron. **26**, 760 (1990).

[62] I. Kang, T. Krauss, and F. Wise, Opt. Lett. **22**, 1077 (1997).

[63] C. H. Kwak, Y. L .Lee, and S. G. Kim, J. Opt. Soc. Am. B **16**, 600 (1999).

[64] M. Falconieri, J. Opt. A: Pure Appl. Opt. **1**, 662 (1999).

[65] S. Alves, A. Bourdon, and A. M. Figueiredo Neto, J. Opt. Soc. Am. B **20**, 713 (2003).

[66] J. Wang, M. Sheik-Bahae, A. A. Said, D. J. Hagan, and E. W. Van Stryland, J. Opt. Soc. Am. B **11**, 1009 (1994).

[67] J. M. Harbold, F. Ö. Ilday, F. W. Wise, J. S. Sanghera, V. Q. Nguyen, L. B. Shaw, and I. D. Aggarwal, Opt. Lett. **27**, 119 (2002).

[68] B. L. Wehrenberg, C. Wang, and P. Guyot-Sionnest, J. Phys. Chem. B **106**, 10634 (2002).

[69] S. F. Wuister, C. de Mello Donega, and A. Meijerink, J. Chem. Phys. **121**, 4310 (2004).

[70] J. H. Warner, E. Thomsen, A. R. Watt, N. R. Heckenberg, and H. Rubinsztein-Dunlop, Nanotechnology **16**, 175 (2005).

[71] C. R. Kagan, C. B. Murray, M. Nirmal and M. G. Bawendi, Phys. Rev. Lett. **76**, 1517 (1996).

[72] C. R. Kagan, C. B. Murray, and M. G. Bawendi, Phys. Rev. B **54**, 8633 (1996).

[73] S. A. Crooker, J. A. Hollingsworth, S. Tretiak, and V. I. Klimov, Phys. Rev. Lett. **89**, 186802 (2002).

[74] I. L. Medintz, A. R. Clapp, H. Mattoussi, E. R. Goldman, B. Fisher, and J. M. Mauro, Nature Materials **2**, 630 (2003).

[75] M. Achermann, M. A. Petruska, S. Kos, D. L. Smith, D. D. Koleske, and V. I. Klimov, Nature **429**, 642 (2004).

[76] S. Kos, M. Achermann, V. I. Klimov, and D. L. Smith, Phys. Rev. B **71**, 205309 (2005).

[77] M. Anni, L. Manna, R. Cingolani, D. Valerini, A. Creti, and M. Lomascolo, Appl. Phys. Lett **85**, 4169 (2004).

[78] R. C. Powell and R. G. Kepler, Phys. Rev. Lett. **22**, 636 (1969).

[79] P. Wu and L. Brand, Anal. Biochem. **218**, 1 (1994).

[80] R. M. Clegg, Curr. Opin. Biotechnol. **6**, 103 (1995).

[81] T. Förster, Discuss. Faraday Soc. **27**, 7 (1959).

[82] R. D. Schaller and V. I. Klimov, Phys. Rev. Lett. **92**, 186601 (2004).

[83] B.-R. Hyun and S. Jacob (private communication).